

1 **Cholinium-based Ionic Liquids as an Efficient Media for Improving the Structural and**  
2 **Thermal Stability of Immunoglobulin G Antibodies**

3 Diksha Dhiman<sup>1</sup>, Meena Bisht<sup>1</sup>, Ana P. M. Tavares<sup>2</sup>, Mara G. Freire<sup>2\*</sup> and Pannuru Venkatesu<sup>1\*</sup>

4 <sup>1</sup>Department of Chemistry, University of Delhi, Delhi-110 007, India

5 <sup>2</sup>CICECO-Aveiro Institute of Materials, Department of Chemistry, University of Aveiro, 3810-  
6 193 Aveiro, Portugal

7 **ABSTRACT:** Among antibody-based biopharmaceuticals, immunoglobulin G (IgG) plays a  
8 central role. However, IgG is a protein and as such easily loses stability, thus compromising its  
9 use as an effective therapeutic. To overcome this drawback, in this work, we evaluated  
10 cholinium-based ionic liquids (ILs) as effective stabilizers of IgG. We have investigated four ILs  
11 in aqueous solution, namely cholinium acetate ([Ch][Ac]), cholinium chloride ([Ch]Cl),  
12 cholinium dihydrogen citrate ([Ch][Dhc]) and cholinium dihydrogen phosphate ([Ch][Dhp]). We  
13 used a quantitative approach using different spectroscopic and chromatographic techniques to  
14 evaluate the thermal and structural stability of IgG. Thermal fluorescence spectroscopy studies  
15 were performed to obtain the transition temperature ( $T_m$ ) and the change in Gibbs free energy  
16 ( $\Delta G$ ) of IgG in all cholinium-based ionic liquid (IL) aqueous solutions. The results indicate an  
17 appreciable increase in  $T_m$  in presence of [Ch][Ac] and [Ch]Cl. The thermodynamic parameters  
18 obtained from thermal fluorescence are compared with the structural stability of IgG by UV,  
19 fluorescence, CD and FT-IR spectroscopies, as well as with SE-HPLC and SDS-PAGE, showing  
20 that all results are in good agreement. Furthermore, the hydrodynamic diameter ( $d_H$ ) of the IgG  
21 as a function of the concentration of IL was analyzed using dynamic light scattering (DLS),  
22 showing favorable interactions between protein residues. Finally, molecular docking studies for  
23 IgG in ILs using Molegro Virtual Docker (MVD) have been performed, reinforcing the main  
24 interactions ruling the IgG stability. This work highlights the potential validity of using  
25 cholinium-based ILs in IgG formulations for enhancing its thermal and structural stability, and  
26 thus preservation of IgG antibodies.

1 **Key words:** Antibodies, Cholinium-based Ionic liquids, Immunoglobulin G, Structural stability,  
2 Thermal stability

3

#### 4 **INTRODUCTION**

5 Antibodies are proteins naturally present in mammal's serum, being of high relevance for  
6 therapeutic purposes.<sup>1</sup> In particular, immunoglobulin G (IgG) is an antibody and a glycoprotein  
7 present in plasma and extracellular fluids, which constitute the humoral branch of the animal  
8 immune system.<sup>2</sup> IgG is a large molecule with a molecular mass of approximately 150 kDa. It  
9 consists of four peptide chains composed of two heavy (H, 50 kDa) and two light (L, 25 kDa)  
10 providing Y-shape confirmation.<sup>3</sup> IgG contains two fragments; the site that can bind to antigens  
11 is called the F<sub>ab</sub> fragment and the site which acts as a base of the protein is known as the Fc  
12 fragment of IgG.<sup>4</sup> Polyclonal IgG obtained from human serum is currently used as IgIV  
13 (immunoglobulin intravenous) solutions to treat several disorders and immunodeficiency.<sup>5,6</sup> On  
14 the other hand, monoclonal IgG antibodies can be obtained through mammalian cell cultures and  
15 recombinant technology, requiring the transfection of cells and culture media.<sup>7</sup> The main reasons  
16 for the increasing popularity of IgG as therapeutics correspond to their specific binding and few  
17 side effects. Furthermore, antibodies may be conjugated to another therapeutic entity for efficient  
18 delivery to a target site, thus reducing potential side effects.<sup>8</sup> However; the widespread use of  
19 IgG is still challenging due to the difficulty in maintaining antibody stability over time to  
20 guarantee therapeutic efficacy when called upon.

21

22 IgG is a protein of very high molecular mass and therefore, is a large and complex molecule,  
23 thus, sustaining inherited physicochemical complexity as compared to small pharmaceutical  
24 molecules.<sup>3</sup> Proteins are highly labile molecules, which may suffer degradation under conditions  
25 that do not correspond to their native environment, such as by changing the pH, ionic strength,  
26 temperature, etc. However, to have therapeutic efficiency, IgG must be highly stable. Therefore,  
27 there is a crucial need for developing novel cost-effective methods to maintain its stability and  
28 biological activity in the available formulations. It is well-known that the solvent formulation has  
29 a key role in maintaining the hugely variable complex of antibodies<sup>9</sup> since the solvent

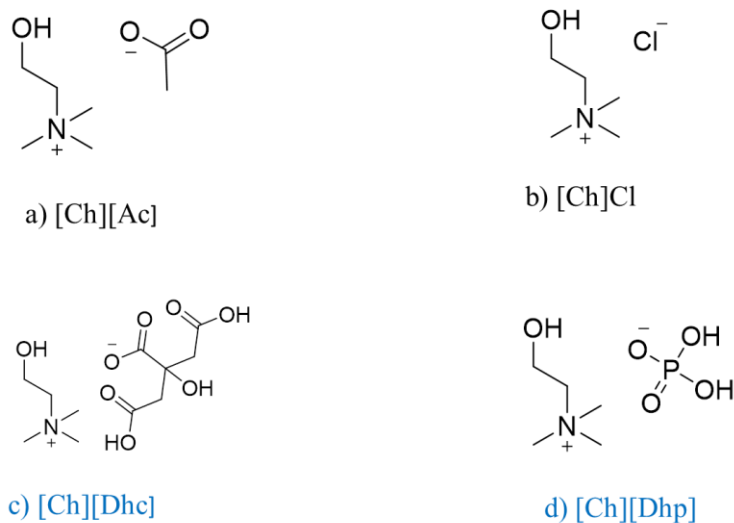
1 surrounding the protein causes differences in electrostatic and hydrophobic interactions.  
2 Furthermore, protein-solvent interactions are equally important as protein-protein interactions,  
3 leading to a large variance in the thermal stability and higher-order structure of proteins.<sup>10</sup> The  
4 critical destabilizing factors that limit the therapeutic use of antibodies are the change in the  
5 structure of the protein in the presence of water as a solvent.<sup>11</sup> As we know, water is a natural  
6 media for vaccine transportation but unfortunately water is not independent of the effect of the  
7 temperature.<sup>11</sup> Therefore, we want to explore the effect of solvents on antibodies which can  
8 behave as excipients and helps with the stabilization of the antibodies in the presence of water.

9 Numerous solvents have been investigated as excipients in formulations to improve the stability  
10 of IgG, however, most of its effective therapeutic utilization; however, most of these solvents  
11 may not be suitable for biomedical applications or do not confer enough stability on these  
12 biopharmaceuticals.<sup>12</sup> In this field, IgG stability might be improved by employing ionic liquids  
13 (ILs) as protective media, while envisioning their use as excipients in IgG formulations. ILs are  
14 molten salts, consisting of large size cations such as quaternary ammonium, imidazolium,  
15 pyridinium, piperidinium, pyrrolidinium, combined with an anion of weak coordination  
16 properties, for instance, halogen, fluorinated or alkyl chain substituents.<sup>13</sup> Compared to  
17 conventional organic solvents, ILs have found widespread applications due to their superior  
18 physical and chemical properties and remarkable solvating power.<sup>12</sup> However, the studies  
19 showed that ILs with larger anions possess higher hydrophobicity and hence high toxicity levels  
20 whereas, the smaller anionic moieties, such as acetate and chloride decrease the toxicity.<sup>14</sup>  
21 Although all the cholinium-based ILs are treated as harmless liquids, Ventura et al. have  
22 demonstrated the increasing trend of eco-toxicity where [Ch][Dhc] is found to be the toxic,  
23 whereas [Ch][Ac] is found better with respect to toxicity index as compared to other cholinium-  
24 based ILs.<sup>15</sup> Clearly, the anion Dhc has longer chain as compared to acetate which can be  
25 responsible for more toxic behavior of larger anion. Aiming at designing excipients that may  
26 increase the stability of antibody-based pharmaceuticals and extend their self-life, cholinium-  
27 based ILs were chosen in this work. Cholinium-based ILs, if properly selected, have high  
28 biocompatibility and biodegradability<sup>16,17</sup>, and they have been proved to be efficient co-solvents  
29 for different proteins, like stem bromelain and cytochrome C. Kumar et al.<sup>18</sup> have demonstrated  
30 that the concentration range of cholinium-based ILs has a high impact on the overall stability of

1 proteins. It has also been shown that chaotropic cation (cholinium) and various kosmotropic  
2 anions of ILs show excellent properties to stabilize the native structure of  $\alpha$ -chymotrypsin.<sup>19</sup>  
3 Furthermore, bio-based cholinium-based ILs have been used for the extraction and purification  
4 of IgG, with the stability of IgG confirmed after the extraction step.<sup>20</sup>  
5 Hallett and co-workers<sup>21</sup> recently studied the effect of different excipients in the presence and  
6 absence of cholinium dihydrogen phosphate ([Ch][Dhp]) on the physical and thermal stability of  
7 IgG. The authors showed that the propensity of IgG for conformational change is driven by the  
8 preferential binding of dihydrogen phosphate anion to the antibody fragment. They further  
9 concluded that formulations containing [Ch][Dhp] with sugars, amino acids and surfactants are  
10 promising candidates for stabilizing IgG against conformational destabilization and aggregation.  
11 Ramalho et al.<sup>22</sup> have also separated IgG using an aqueous biphasic system (ABS) composed of  
12 cholinium-based ILs, finding that in all ABS, IgG preferentially partitions to the IL-rich phase,  
13 unveiling preferential interactions between IgG and cholinium-based ILs. Although all these  
14 shreds of evidence show that formulations composed of cholinium-based ILs may be promising  
15 candidates to improve the stability, more biophysical studies are still needed to confirm their true  
16 potential as excipients in IgG formulations.

17 In this work, we have studied the impact of cholinium-based ILs at different concentrations on  
18 IgG. The thermal and structural stabilities of IgG were explored using various biophysical  
19 techniques, such as UV-visible, steady-state fluorescence, thermal fluorescence, circular  
20 dichroism (CD) spectroscopy, Fourier-transform infrared spectroscopy (FTIR), size exclusion  
21 high performance liquid chromatography (SE-HPLC), sodium dodecyl-sulfate polyacrylamide  
22 gel electrophoresis (SDS-PAGE) and dynamic light scattering (DLS). We are trying to analyze  
23 the effect of ILs on the hydration layer of IgG. We have also studied the time-dependent stability  
24 of IgG in the presence of ILs which further explores the effect of ILs for storage of IgG in the  
25 presence of ILs. Ultimately these results provide the useful information regarding the  
26 stabilization of antibodies and increasing packaging and storage capabilities of IgG in presence  
27 of cholinium-based ILs.<sup>23</sup>The applied methodology allowed us to deliver key insights into the  
28 impact of cholinium-based ILs on the structural and thermal stability of IgG. The data obtained  
29 will help researchers to design better excipients to improve the structural and thermal stability of  
30 IgG and other biopharmaceuticals. Figure 1 shows the chemical structure of the studied  
31 cholinium-based ILs.

1



2 **Figure 1.** Chemical structure of the investigated cholinium-based ILs a) [Ch][Ac] b) [Ch]Cl c)  
3 [Ch][Dhc] d) [Ch][Dhp].

#### 4 MATERIALS AND METHODS

5 IgG from human serum (reagent grade  $\geq 95\%$ ) was purchased, as a lyophilized powder, from  
6 Sigma Aldrich, USA. Cholinium acetate  $\geq 95\%$  and cholinium dihydrogen citrate  $\geq 98\%$  were  
7 also purchased from Sigma Aldrich, USA. cholinium chloride,  $\geq 98\%$ , was purchased from Alfa  
8 Aesar and cholinium dihydrogen phosphate,  $>98\%$  was purchased from Lolitech company. The  
9 water content of all ILs were measured using a Metrohm 831 Karl Fisher coulometer (Table S1)  
10 to guarantee the correct concentration of ILs. Moreover the pH values of all ILs are also included  
11 in Table S1.

12 Sodium phosphate buffer pH 7.0 (10 mM) was used as a reference solvent for preparing IgG  
13 solution and ILs solutions in double-distilled water. The IgG concentration was fixed to 3.0  $\mu\text{M}$   
14 for all measurements, except for the DLS measurements in which the IgG concentration was kept  
15 at 1.5 mM. The concentration of IgG was confirmed by UV visible spectroscopy using an  
16 extinction coefficient of 1.41  $\text{cm}^2/\text{mg}$ . The stock concentration of all the ILs taken was 5 mM,

1 which was further diluted from 0.5 to 2.5 mM. All samples were incubated for 15–20 min at 25  
2 °C in order to attain equilibrium.

### 3 **INSTRUMENTATION AND MEASUREMENTS**

4 The UV absorption spectra of IgG 3.0 μM consisting of sodium phosphate buffer pH 7.0, 10 mM  
5 and various concentrations of ILs (0.5-2.5 mM) were measured by Shimadzu UV-1800 (Japan)  
6 spectrophotometer with the highest resolution (1 nm) in a wavelength range of 200–350 nm  
7 using quartz cells of path length 1 cm at 25 °C.

8 SE-HPLC (Chromaster, VWR Hitachi) equipped with a size exclusion column (Shodex Protein  
9 KW-802.5; 8 mm x 300 mm) and DAD detector was used to evaluate the  
10 aggregation/degradation of IgG structure by changes in the retention time. The samples consisted  
11 of IgG 3.0 μM pH 7.0 buffer (control) with different concentrations of ILs (0.5-2.5 mM). The  
12 mobile phase consisted of 10 mM sodium phosphate buffer pH 7.0 and NaCl 0.3 M. The sample  
13 injection volume was 25 μL and the wavelength was set at 280 nm. The samples ran isocratically  
14 with a flow rate of 0.5 mL.min<sup>-1</sup>. The autosampler and column oven were kept at 10 and 40 °C,  
15 respectively.

16 The structural stability of IgG was also evaluated by SDS-PAGE. All samples containing IgG 3.0  
17 μM in sodium phosphate buffer pH 7.0, 10 mM in the presence of various concentrations of ILs  
18 (0.5-2.5 mM) were diluted in Laemmli sample buffer with dithiothreitol (DTT) (reduced  
19 conditions). The effect was to load ca. 200 μg of IgG per mL per lane prior to loading in the gel  
20 wells. These solutions were heated at 95 °C for 5 min for denaturation followed by loading into  
21 the wells of the SDS-PAGE gel containing 20% polyacrylamide. SDS-PAGE molecular weight  
22 markers from VWR were used. Gels were electrophoresed for 1.5 h at 135 V on polyacrylamide  
23 gels (stacking 4%; resolving 20%) with a running buffer constituted by 250 mM Tris-HCl, 1.92  
24 M glycine and 1% SDS. After the run, the gels were stained with Coomassie Brilliant Blue G-  
25 250 0.1% (w/v), methanol 50% (v/v), acetic acid 7% (v/v) and water 42.9% (v/v) for 3–4 h at  
26 room temperature in an orbital shaker. The gels were then de-stained in a solution of acetic acid  
27 at 7% (v/v), methanol at 20% (v/v) and water at 73% (v/v) in an orbital shaker at 50 rpm for 3–4  
28 h at 40 °C.

1 A Cary Eclipse spectrofluorometer from Varian optical spectroscopy instruments (Mulgrave,  
2 Victoria, Australia) equipped with a thermostat cell holder was used to monitor the fluorescence  
3 emission spectra of 3.0  $\mu\text{M}$  IgG in 10 mM sodium phosphate buffer at pH 7.0 and in the presence  
4 of various concentrations of ILs (0.5-2.5 mM). The excitation wavelength was set at 275 nm and  
5 the emission spectra recorded were between 280 to 400 nm in order to calculate the contribution  
6 of the tyrosine (Tyr) residue to the overall fluorescence emission.<sup>24</sup> The slit widths for excitation  
7 and emission were being set at 5 nm. The thermal stability of IgG in sodium phosphate buffer as  
8 a function of the concentration of ILs (0.5-2.5 mM) was analyzed by the fluorescence spectra  
9 from 20 to 90 °C at an exciting wavelength of 275 nm. A 1 cm path length cuvette was used for  
10 the thermal unfolding analysis. The temperature was increased at a heating rate of 2 °C/min  
11 using the peltier thermocouple and a time constant of 16 s. All the unfolding transitions of the  
12 IgG were determined by employing the two-state unfolding mechanism.

13 The Far-UV CD measurements of IgG 3.0  $\mu\text{M}$  in 10 mM sodium phosphate butter at pH 7 and as  
14 a function of the concentration of ILs (0.5-2.5 mM) carried out at 25 °C using the Jasco J-815  
15 spectrophotometer with a quartz cuvette of the path length of 0.1 cm at 25 °C. The wavelength  
16 range was set from 190 to 240 nm at 25 °C. The other parameters which were fixed are response  
17 time, 1 s; bandwidth, 1 nm and scan rate, 50 nm/min. The spectrum of the buffer alone was taken  
18 and was deducted from the final scan, functioning as a baseline correction.

19

20 Fourier-transform infrared (FTIR) spectra of IgG in the absence and presence of various  
21 concentrations of ILs (0.5, 1, 1.5, 2.5mM) were recorded by using an IRAffinity-1S  
22 SHIMADZU FTIR spectrometer. The FTIR spectra were obtained in the wavenumber range of  
23 4000-400  $\text{cm}^{-1}$  by accumulating 256 scans, with a resolution of 4  $\text{cm}^{-1}$  in transmittance mode. All  
24 samples were prepared in a  $\text{D}_2\text{O}$  buffer. The concentration of IgG was 3 $\mu\text{M}$ .

25 The hydrodynamic diameter ( $d_{\text{H}}$ ) of IgG at a concentration of 1.5  $\mu\text{M}$  in (10 mM, pH =  
26 7.0) sodium phosphate buffer was determined as a function of the concentration in sodium  
27 phosphate buffer pH 7.0, 10 mM was measured as a function of the concentration of ILs (0.5-2.5  
28 mM). The DLS was of the company Zetasizer Nano instrument (ZS90), (Malvern Instruments

1 Ltd., UK), equipped with He-Ne laser (4 mW, 632.8 nm). The scattering angle was set to 90°  
2 with a fixed operating wavelength of 633 nm.

3 Molecular docking was performed to find out the potential binding site of ILs F<sub>ab</sub> and F<sub>c</sub>  
4 fragments of IgG. The trial version of Molegro virtual docker (MVD) was downloaded from  
5 Molegro to carry out the docking studies. All the default parameters were set. Three-dimensional  
6 structures of Fab (light and heavy chain) and Fc fragments of IgG were acquired from the RCSB  
7 in protein databank format (PDB entry 1N0X and 4BYH, respectively). Yasara online available  
8 software was used for optimizing the energy of both the fragments. For structure preparation and  
9 energy minimization, Chem Draw and Chem Draw 3D were used. The binding sites were  
10 restricted to the sphere of the radius of 15 Å, and all the other parameters including the  
11 maximum (1500 A) of the size iterations, a number of runs 60, maximum population size (60),  
12 scaling factor 0.5, grid resolution 0.30, and crossover rate 0.9, were fixed.

13

## 14 **RESULTS AND DISCUSSION**

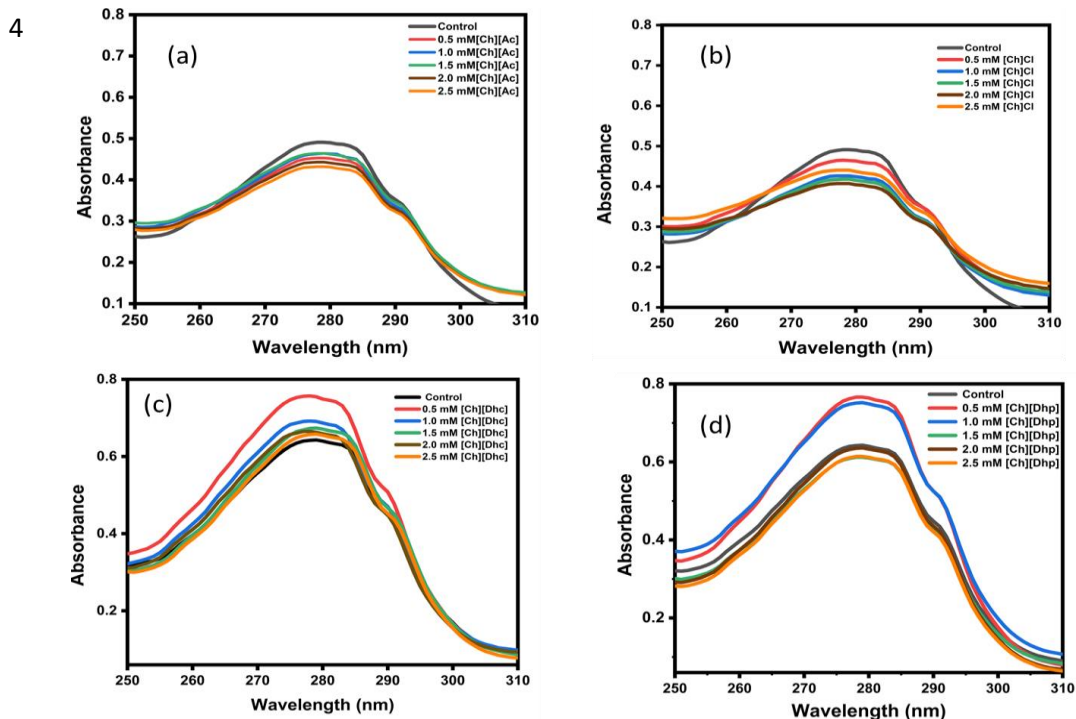
### 15 **Effect of Cholinium-Based ILs on the Structure of IgG as a function of concentration and** 16 **the nature of anion**

17 Up to date, the mechanisms of IgG behavior and a complete study of its structural and thermal  
18 stabilities in the presence of a wide range of cholinium-based ILs ([Ch][Ac], [Ch]Cl, [Ch][Dhc],  
19 and [Ch][Dhp]) has not previously been investigated. In this work, we have tried to explore the  
20 interactions between cholinium-based ILs and IgG, by applying a series of biophysical  
21 techniques, thus we can investigate the potential of these ILs to act as potential excipients to  
22 preserve IgG biopharmaceuticals. In addition, our examination of the temperature derived  
23 folding/unfolding has been carried out as a function of a concentration gradient. Overall,  
24 different ILs may have different significance, which is established by the physical and chemical  
25 properties of each IL in relation to the protein under study.

26 **UV Spectral Analysis.** UV absorption measurement is a successful method to explore  
27 conformational changes of proteins. Figure 2 shows the absorption spectra of IgG in the presence  
28 of various concentrations of cholinium-based ILs (0.5-2.5 mM) at 25 °C. The maximum



1 wavelength ( $\lambda_{\max}$ ) for the absorbance maxima of IgG is observed at 280 nm. The peak around  
2 280 nm is due to the absorption of aromatic residues such as tryptophan (Trp), tyrosine (Tyr) and  
3 phenylalanine (Phe).<sup>24,26</sup>



5 **Figure 2.** UV absorption spectra analysis of IgG at 25 °C in the presence of sodium phosphate  
6 buffer pH 7.0, 10 mM (control) and at various concentrations of ILs: (a) [Ch][Ac], (b) [Ch]Cl,  
7 (c) [Ch][Dhc], (d) [Ch][Dhp].

8  
9 From Figure 2, UV absorbance results suggest that IgG shows a lead hypochromic (Figure 2 a  
10 and b) and hyperchromic (Figure 2c and d) shift in presence of ILs. As can be seen in Figure 2a,  
11 the  $A_{\max}$  of IgG slightly decreases (Table S2) with the increasing concentration of [Ch][Ac],  
12 which indicates that the aromatic residues of IgG may not be significantly exposed to the solvent,  
13 resulting in a lower absorbance. In the case of [Ch]Cl (Figure 2b) the absorbance of IgG first  
14 decreases up to 2.0 mM, and then starts to increase at 2.5 mM (Figure 2b, Table S2). However,  
15 this increase is lower than in the control (IgG in phosphate buffer). On the other hand, in the  
16 presence of [Ch][Dhc] and [Ch][Dhp] (Figures 2c and 2d) IgG shows a sharp increase in the  
17 absorbance values at lower IL concentrations (0.5 and 1 mM), and then the absorbance decreases

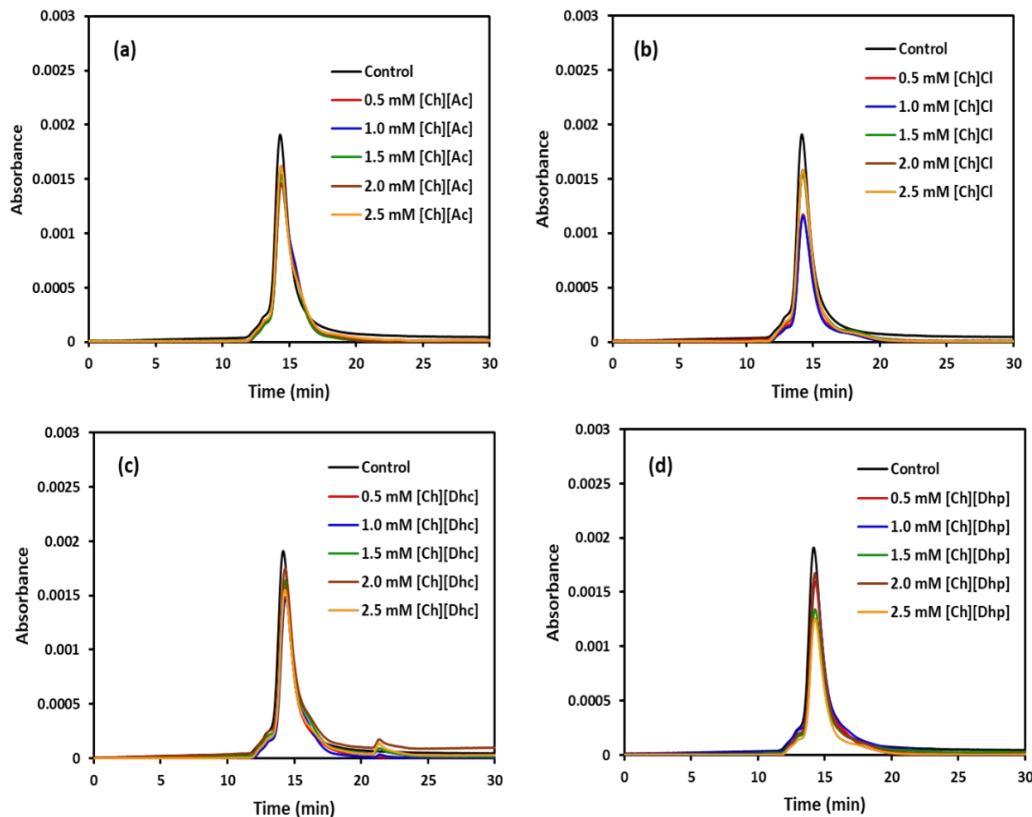
1 as the concentration of [Ch][Dhp] and [Ch][Dhc] increases (Table S2). This trend indicates  
2 protection of aromatic residues of IgG at higher concentrations of [Ch][Dhp] and [Ch][Dhc].  
3 Interestingly, there is no alteration in the  $\lambda_{\max}$  of IgG in all the studied concentration of ILs  
4 (Table S2). Hence, from UV studies it can be assumed that the IgG can sustain a more compact  
5 conformation in these ILs as compared to that in the buffer solution.

6 **SE-HPLC Analysis.** The structural changes of IgG were evaluated by SE-HPLC. Even though  
7 SE-HPLC may be used to quantify IgG, and identify and quantify the presence of other proteins,  
8 this method can be used to evaluate the structure of antibodies since peaks corresponding to  
9 proteins aggregation or fragmentation will appear in the respective chromatograms.<sup>20,22,25</sup> The  
10 importance of evaluating the presence of IgG aggregates is due to its biological activity, which is  
11 related to the therapeutic efficiency that is usually reduced by the formation of aggregates.<sup>25</sup>  
12 Moreover, IgG aggregation may be fatal for patients with a variety of diseases involving protein  
13 aggregation.<sup>22</sup>

14 SE-HPLC chromatograms of IgG in the presence of sodium phosphate buffer pH 7.0, 10 mM  
15 (control) and at various concentrations of the ILs [Ch][Ac], [Ch]Cl, [Ch][Dhc] and [Ch][Dhp]  
16 are shown in Figure 3. According to the obtained results, under the chromatographic conditions  
17 applied, IgG samples show 2 peaks: one peak at a retention time of ~14.3 min, corresponding to  
18 the IgG in its monomeric form, and a second peak at ~13.4 min, indicating the presence of some  
19 IgG aggregates present in the commercial IgG from human serum. Compared to the control  
20 sample in buffer, after the IgG incubation in all cholinium-based ILs, showed no increase in  
21 protein aggregates, implying that these cholinium-based ILs have a good potential to avoid IgG  
22 aggregation. Additionally, no shift in the retention time is observed for all samples and no peaks  
23 at higher retention times are observed, meaning that no IgG degradation occurs. In a previous  
24 study reporting the use of 1-alkyl-3-methyl imidazolium chloride (alkyl: ethyl, butyl, hexyl and  
25 octyl), it was found that ILs were able to dissociate IgG aggregates, being 1-ethyl-3-  
26 methylimidazolium chloride the best solvent towards this end.<sup>25</sup> In a similar work, the  
27 aggregation of IgG was studied in the presence of different concentrations of 1-octyl-3-  
28 methylimidazolium chloride, and it was found upon increasing IL concentrations from 0.05 to  
29 0.20% w/v that the size of the non-aggregated fraction was invariant at different pH values.<sup>25</sup>  
30 These findings are in agreement with the stability of other model proteins (hen egg white

1 lysozyme and the single-chain antibody fragment ScFvOx) in the presence of imidazolium-based  
2 ILs, where the selected ILs suppress protein aggregation.<sup>26</sup>

3



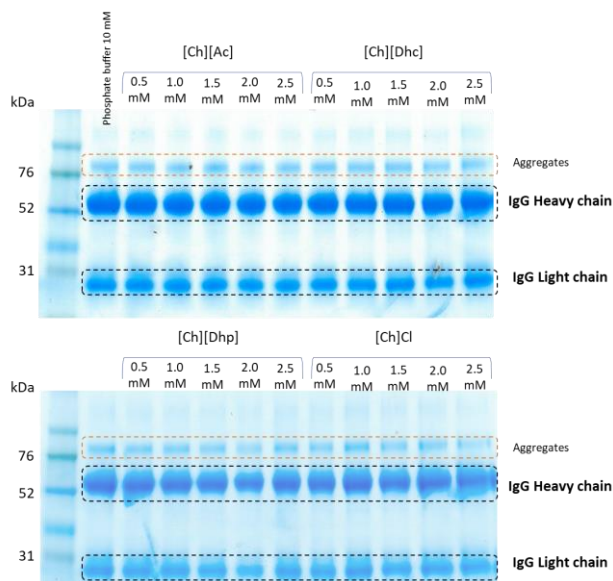
4 **Figure 3.** SE-HPLC chromatograms of IgG in the presence of phosphate buffer pH 7.0, 10 mM  
5 (control) and in the presence of cholinium based-ILs at various concentrations: (a) [Ch][Ac], (b)  
6 [Ch]Cl, (c) [Ch][Dhc], (d) [Ch][Dhp].

7

8 **SDS-PAGE Analysis.** The structural stability of IgG in the presence of [Ch][Ac], [Ch][Dhc],  
9 [Ch][Dhp] and [Ch]Cl at different concentrations (0.5- 2.5 mM) was evaluated by SDS-PAGE,  
10 whose results are displayed in Figure 4. SDS-PAGE for IgG in sodium phosphate buffer (10  
11 mM, pH 7.0; control) was performed for comparative analysis. According to the SDS-PAGE in  
12 reduced conditions, control IgG is composed of 2 heavy chains with a molecular weight of ~ 50  
13 kDa and 2 light chains with a molecular weight of ~ 25 kDa (Figure 4). These two bands are

1 identified in the presence of all cholinium-based ILs investigated and at all concentrations,  
2 indicating that there are no changes and no degradation of the IgG structure. Moreover, as  
3 verified by the SE-HPLC chromatograms, a band with high molecular weight is observed,  
4 indicating the presence of IgG agglomerates in the control and IL solutions. However, the  
5 intensity of this band is not observed to increase, thus corroborating the SE-HPLC results, *i.e.*, no  
6 new IgG aggregates other than originally present are formed.<sup>28,29</sup> In the previous studies the  
7 structural stability of IgG was evaluated in presence of imidazolium-, ammonium- and  
8 phosphonium-based ILs by SDS-PAGE, after its extraction from rabbit serum, no degradation of  
9 IgG was detected, except in presence of tetrabutylphosphonium bromide. In this previous work,  
10 Ferreira et al.<sup>30</sup> concluded that the high hydrophobicity of phosphonium-based ILs was the main  
11 reason behind its stronger negative effect on the integrity of IgG. These and the current results  
12 combine to reinforce the conclusion that cholinium- based ILs, by being more hydrophilic,  
13 behave as more suitable and biocompatible media for keeping the IgG structure stable<sup>31,32</sup>.

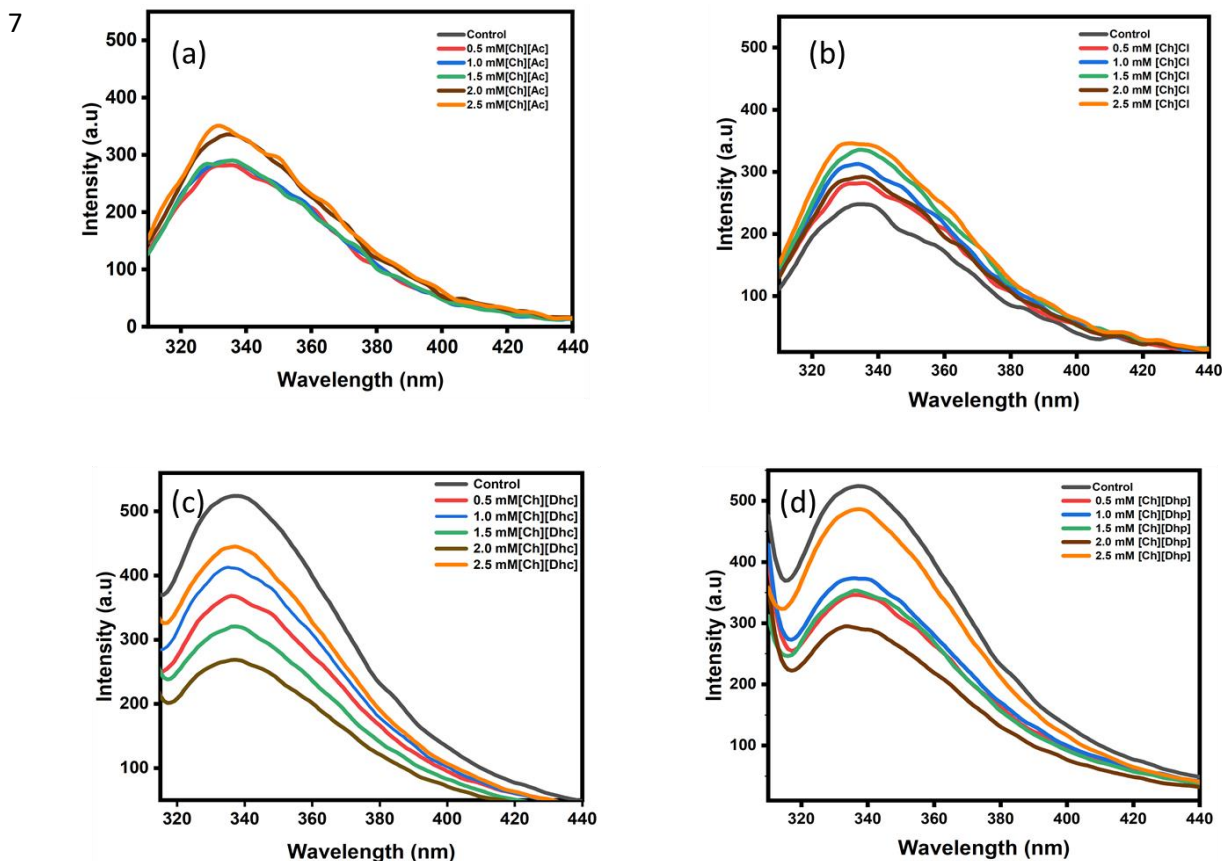
14



15 **Figure 4.** SDS-PAGE of IgG at different concentrations of [Ch][Ac], [Ch][Dhc], [Ch][Dhp] and  
16 [Ch]Cl. Lane 1 – molecular weight marker; lane 2 – IgG in sodium phosphate buffer pH 7.0, 10  
17 mM (control).

18

1 **Steady-State Fluorescence Spectral Analysis.** The aromatic amino acids Trp, Tyr, and Phe  
2 serve as intrinsic fluorescence probes to study protein conformation, dynamics, and  
3 intermolecular interactions. The fluorescence properties such as maximum intensity ( $I_{max}$ ) and  
4 maximum emission wavelength ( $\lambda_{max}$ ) are highly sensitive to the polarity change in the  
5 microenvironment around the aromatic residues that can be used to investigate IgG–IL  
6 interactions.<sup>17</sup>



8 **Figure 5.** Fluorescence spectra analysis of IgG at 25 °C in the presence of phosphate buffer  
9 (pH=7) and various concentrations of ILs: (a) [Ch][Ac], (b) [Ch]Cl, (c) [Ch][Dhc], and (d)  
10 [Ch][Dhp].

11 Figure 5 reveals the variation of emission spectra of IgG in the presence of various  
12 concentrations of different ILs when excited at 275 nm.<sup>24</sup> The change in the Tyr fluorescence is  
13 indicative of disturbance in the conformational dynamics of IgG. As can be clearly observed in  
14 Figure 5, in the case of IgG in [Ch][Ac], the  $I_{max}$  is gradually increasing with the increase in the

1 concentrations whereas in the case of [Ch]Cl the  $I_{max}$  increases with increase in the concentration  
2 of IL except at concentration 2.0 mM (Table S3) ILs do not cause any shift in  $\lambda_{max}$ . The increase  
3 in the intensity can attribute to higher quantum yield (ratio of the photon emitted to photon  
4 absorbed) of IgG in the presence of [Ch][Ac] and [Ch]Cl as fluorophore's environment can  
5 impact quantum yield, usually resulting from changes in the rates of non-radiative decay.<sup>33</sup> On  
6 the other hand, a sharp decrease in the  $I_{max}$  is observed in presence of [Ch][Dhp] (Figure 5d) at  
7 0.5, 1 and 2 mM. A slight increase in  $I_{max}$  was observed on further addition of [Ch][Dhp] (Table  
8 S3). However, this increase is lower when compared to the control value. In the case of  
9 [Ch][Dhc] (Figure 5c), a sharp decrease in the  $I_{max}$  is observed even at the lowest concentration  
10 (0.5 mM) (Table S3), which is an indication of decreased hydrophobicity around the Tyr  
11 residue.<sup>34</sup> Nevertheless, it should be remarked that the trend of fluorescence is not uniform in the  
12 case of [Ch][Dhc] as well as there is no appreciable shift in the  $\lambda_{max}$  value of IgG in the presence  
13 of all ILs. All the values of  $\lambda_{max}$  and  $I_{max}$  are provided in Table S3. From the fluorescence results,  
14 it can be anticipated that Tyr of IgG may be getting exposed to the polar environment in the case  
15 of [Ch][Dhc] and [Ch][Dhp]. Thereby, there is more quenching of Tyr by [Ch][Dhc] and  
16 [Ch][Dhp] in comparison to [Ch][Ac] and [Ch]Cl. This behavior of the protein can be attributed  
17 to either the burial of Tyr inside the core of protein or the decreased quenching by neighboring  
18 charged residues.

19  
20 **Fluorescence Quenching Effect Shown by [Ch][Dhc].** In order to ascertain fluorescence  
21 quenching effect, fluorescence quenching of IgG in the presence of [Ch][Dhc] is studied. The  
22 Stern–Volmer plot of fluorescence Quenching is displayed in Figure 6.

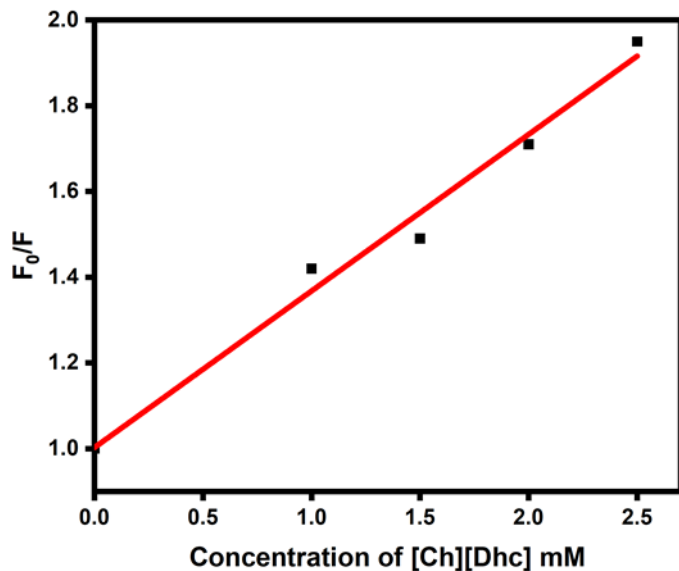


**Figure 6.** Stern–Volmer plot for quenching of IgG fluorophore by [Ch][Dhc]. The black square points represent the  $F_0/F$  values of IgG at various concentrations of [Ch][Dhc] and red line represents the linear curve fit.

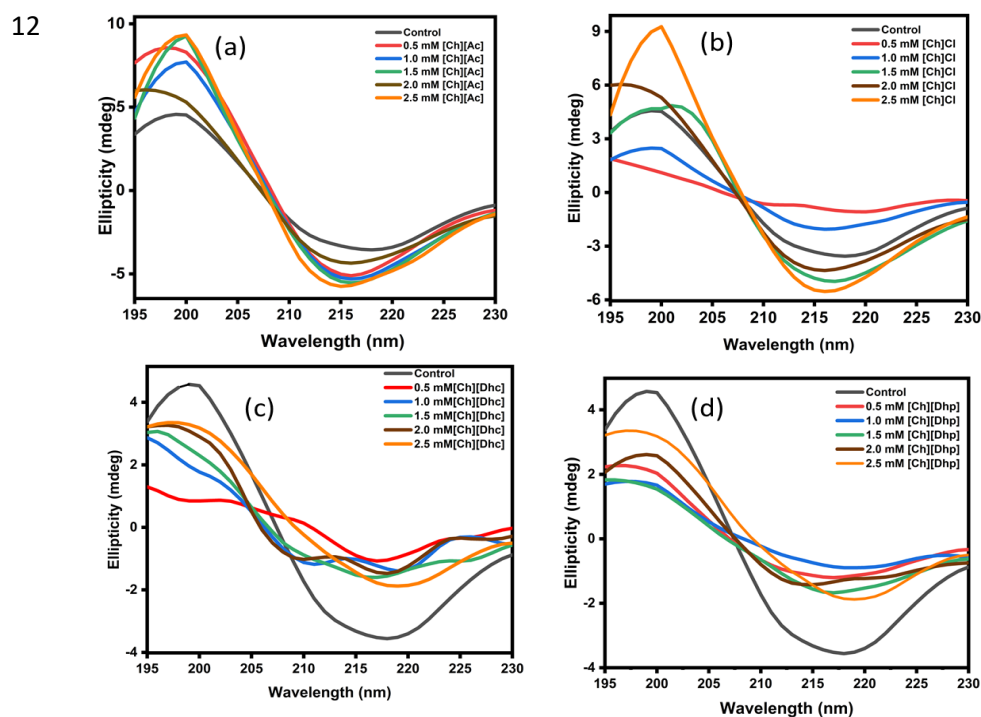
Generally, in fluorescence spectroscopy, two types of quenching are possible, static quenching or dynamic quenching. In static quenching ground state complex form between fluorophore and quencher whereas, in dynamic quenching excited state collision of fluorophore and quencher takes place.<sup>35</sup> Hence, the quenching ability of [Ch][Dhc] is predicted with the help of Stern–Volmer plot which reflects the binding of [Dhc] with protein in the vicinity of fluorophore and protein backbone. The linear relationship between the fluorescence intensity of IgG and the concentration of [Ch][Dhc] is obtained from following equation.

$$F_0/F = 1 + k_{sv} [Q] = 1 + \tau_0 k_q [Q] \quad (1)$$

Where,  $F_0$  is the intensity of fluorophore in the absence of quencher,  $F$  is the intensity of the fluorophore in the presence of quencher,  $[Q]$  is the concentration of the quencher,  $k_q$  is Quenching constant,  $\tau_0$  is average life time of fluorophore that is  $10^{-8}$  and  $k_{sv}$  is calculated from the slope of  $F_0/F$  versus concentration of [Ch][Dhc]. The  $k_{sv}$  values for IgG in the presence of [Ch][Dhc] was obtained from the slope of the Stern–Volmer plot and was found to be  $0.36 \text{ M}^{-1}$  and  $k_q$  values were obtained from average life-time of fluorophore and the value was found  $3.6 \times$

1  $10^7 \text{ s}^{-1}$ . The  $k_q$  value calculated from Stern–Volmer equation was found to be in the order of  $10^7$   
2  $\text{s}^{-1}$  which is less than the maximum dynamic quenching constant value (i.e.,  $2 \times 10^{10} \text{ M}^{-1} \text{ s}^{-1}$ )  
3 revealing that fluorescence quenching of IgG in the presence [Ch][Dhc] arises due to dynamic  
4 diffusion. Hence, it can be concluded that [Dhc] and [Dhp] anions form complex with the excited  
5 tyrosine residue of the protein in the presence of UV absorbance which is responsible for the  
6 quenching in the fluorescence intensity.

7 **CD Spectral Analysis.** To gain more insight into the possible structural changes of IgG, CD  
8 spectroscopy studies were carried to study the changes in the secondary structure of the protein  
9 in the presence of cholinium-based ILs at different concentrations (Figures 7 and 8). Far UV CD  
10 spectra (180-250) can provide qualitative information about the presence of secondary structural  
11 element analysis in the protein.<sup>36</sup>

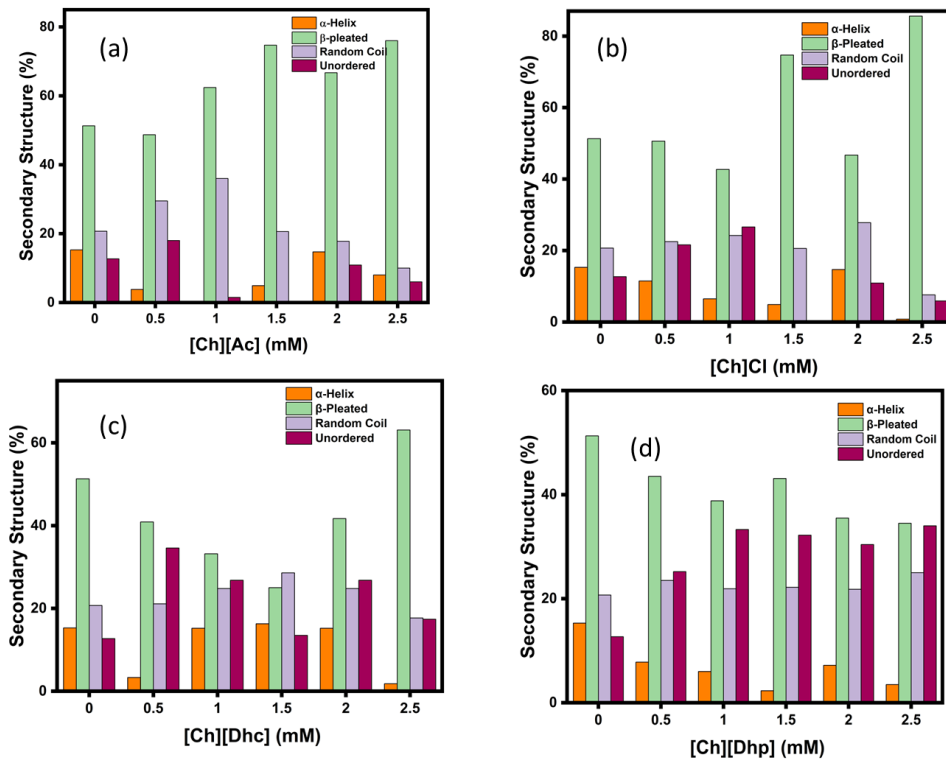


13 **Figure 7.** Far-UV CD analysis of IgG at 25 °C in the presence of phosphate buffer (pH=7.0, 10  
14 mM) and at various concentrations of ILs: (a) [Ch][Ac], (b) [Ch]Cl, (c) [Ch][Dhc] and (d)  
15 [Ch][Dhp].



1 In the Far-UV CD studies, a broad minimum at 218 nm and maximum at 199 nm suggests that  
2 the  $\beta$ -sheet structure dominates in the IgG (Figure 7).<sup>36</sup> As can be seen from Figure 7 (a), both  
3 positive and negative band ellipticity of IgG increases with the addition of [Ch][Ac]. From  
4 Figure 7 (b), it is clear that in presence of [Ch]Cl, the secondary structure of IgG is first disturbed  
5 at lower concentrations (0.5 and 1 mM), while with the increase in concentration (after 1.5 mM)  
6 the negative, as well as positive ellipticity, starts to increase which corresponds to increase in the  
7  $\beta$ -sheeted conformation.<sup>37</sup> However, similar to UV and fluorescence results, contrasting CD  
8 trends occur in the case of [Ch][Dhp] and [Ch][Dhc]. Results in Figure 7 (c) reveal that in  
9 presence of [Ch][Dhc] the secondary structure of IgG is disturbed even at low concentrations.  
10 Nevertheless, at a higher concentration of 2.5 mM, IgG starts to restore its secondary structure.  
11 In Figure 7 (d), it can be observed that with the increase in concentration (up to 1.5 mM) of  
12 [Ch][Dhp], there is a decrease in the ellipticity value with a slight blue shift. A further increase in  
13 concentrations (at 1.0 and 1.5 M) leads to the ellipticity starting to increase, however, but still  
14 lower than in the control. A reduction in the ellipticity indicates partial unfolding through the  
15 conversion of  $\beta$ -sheet into unordered structures. The percentage of secondary structure was  
16 calculated using Dichroweb software and it was concluded that overall, in presence of [Ch][Ac]  
17 and [Ch]Cl (Figures 8a and 8b) the percentage of  $\beta$ -sheet increases as compared to the control.  
18 On the other hand, in presence of [Ch][Dhc] and [Ch][Dhp] (Figures 8c and 8d), there is an  
19 alteration in secondary structure at a concentration lower than 2.5 mM with a reduction of  $\beta$ -  
20 sheet conformations accompanying an increase in unordered structure. In summary, the data  
21 suggest that [Ch][Ac] and [Ch]Cl help in retaining the secondary structure of IgG and to form a  
22 more compact structure at all studied concentrations as compared to [Ch][Dhc] and [Ch][Dhp].

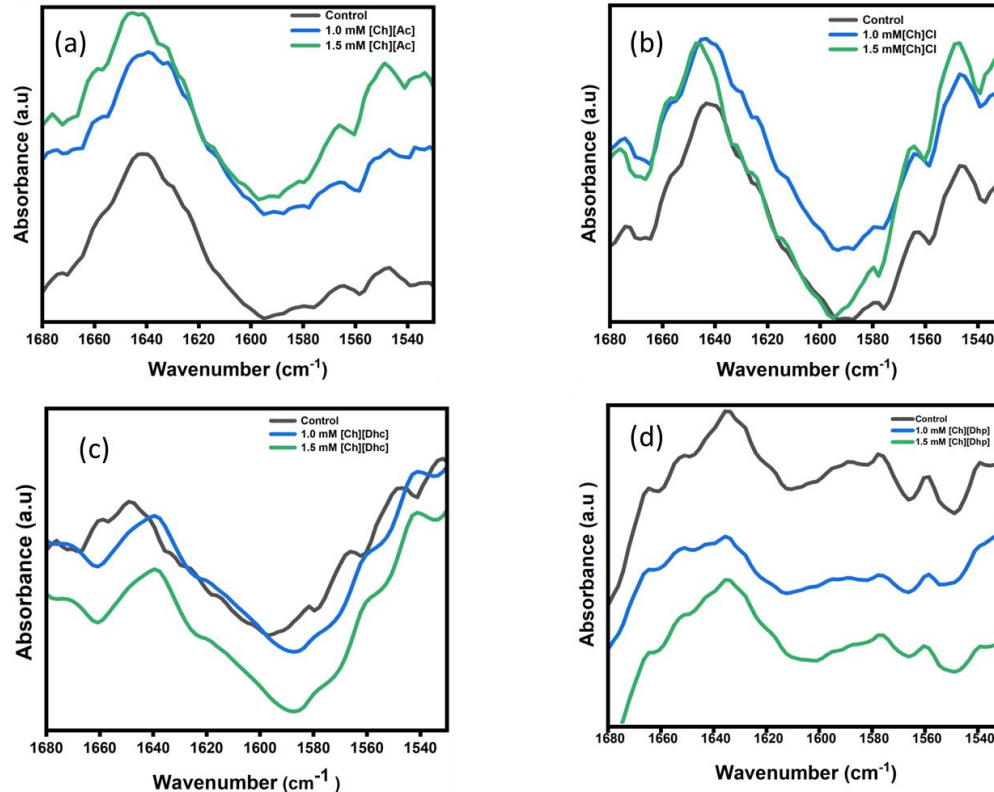
1



2 **Figure 8.** Secondary structure (%) of IgG in presence of varying concentrations of ILs: (a)  
 3 [Ch][Ac], (b) [Ch]Cl, (c) [Ch][Dhp], and (d) [Ch][Dhc].

4 **FT-IR Analysis.** FTIR is concerned with the vibration of molecules absorbing in the infrared  
 5 region of the electromagnetic spectrum. For proteins, the vibrational bands studied are mostly the  
 6 amide I at 1640 and amide II band occurs at 1550  $\text{cm}^{-1}$ . Amide I come in the region of 1625-  
 7 1695  $\text{cm}^{-1}$ , and is primarily due to the amide C=O stretching vibrations of the peptide bonds,  
 8 whereas amide II covers the region 1550  $\text{cm}^{-1}$  due to CN stretching and NH bend.<sup>38</sup> Since the  
 9 vibrational frequency depends upon the bond strength while the intensity depends upon the bond  
 10 polarity, the absorption depends upon the bond vibrations which are excited. The increase in  
 11 bond strength increases the frequency of vibration, whereas the increase in bond polarity  
 12 increases the intensity of absorption.<sup>39</sup>

1

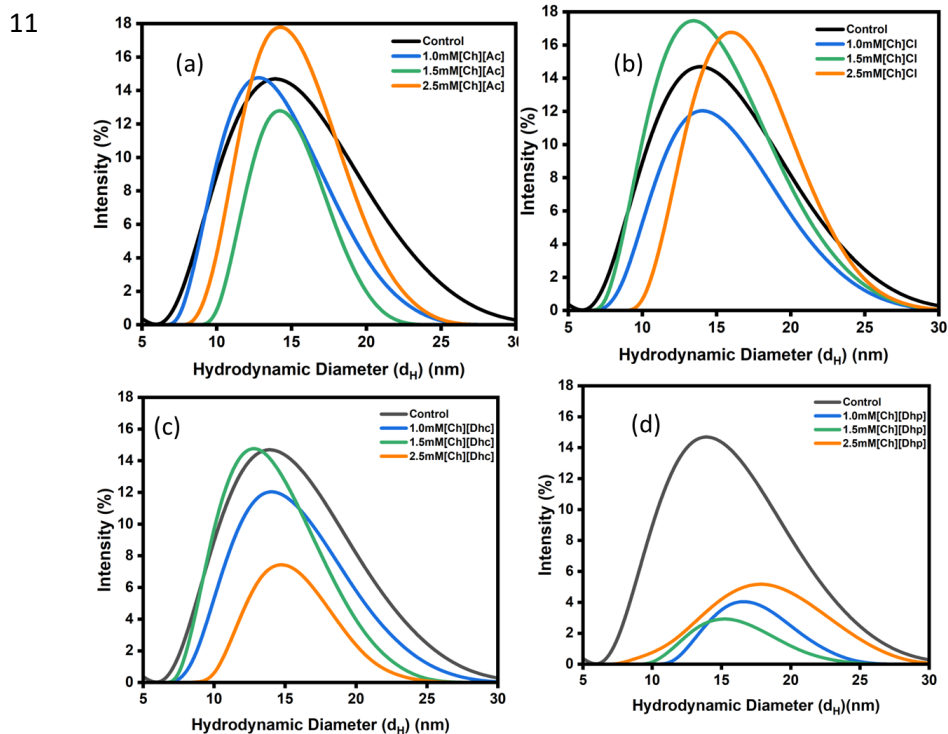


2 **Figure 9.** FTIR spectra of IgG in the amide I and amide II regions at 25 °C in the presence of the  
 3 ILs: (a) [Ch][Ac],(b)[Ch]Cl, (c) [Ch][Dhc] and (d) [Ch][Dhp] at various concentrations. Control:  
 4 IgG in sodium phosphate buffer, pH 7.0, 10 mM.

5 From Figure 9, it can be seen that IgG shows both amide I and amide II bands. Indeed, in the  
 6 presence of [Ch][Ac], with increasing concentration in the absorbance of both bands of IgG with  
 7 the increase in the concentration of [Ch][Ac], which highlights the increase in the polarity of the  
 8 carbonyl and N-H vibrational band due to hydrogen bonding. Similarly, in the presence of  
 9 increasing concentration of [Ch]Cl, the strength of the absorbance of IgG increases (Figure 9b),  
 10 whereas in the presence of [Ch][Dhc] and [Ch][Dhp] the maximum absorbance is shown by the  
 11 control point and then the sequence is in the increasing order of the concentration of the IL  
 12 (Figure 9c and d). Coming to the wavenumber shift, in the presence of [Ch]Cl there is no major  
 13 shift, where as in the presence of [Ch][Dhp] and [Ch][Dhc] the amide I peak of IgG at 1640 cm<sup>-1</sup>  
 14 is shifted towards shorter wavelengths, thus implying an increase in the hydrogen bond  
 15 formation between IgG and [Ch][Dhp] and [Ch][Dhc]. Therefore, it can be concluded that the  
 16 secondary structure of IgG is not altered by the addition of any IL (as both the peaks were

1 retained in all the ILs). Nevertheless, extended hydrogen bonding may be seen in the case of  
2 [Ch][Dhc] and [Ch][Dhp].

3  
4 **Hydrodynamic size studies.** Dynamic light scattering (DLS) is a technique used to calculate  
5 the hydrodynamic diameter ( $d_H$ ) of a molecule.  $d_H$  can be defined as the diameter of a  
6 hypothetical sphere that diffuses at the same rate as the molecule under investigation.<sup>40</sup> Hence, in  
7 order to elucidate the attenuation effects of cholinium-based ILs on IgG, the DLS measurements  
8 were performed as a function of the concentration of the ILs [Ch][Ac], [Ch][Cl], [Ch][Dhc] and  
9 [Ch][Dhp], being the results are illustrated in Figures 10 and 11. Additional data can be found in  
10 Table S4 in the Supporting Information.

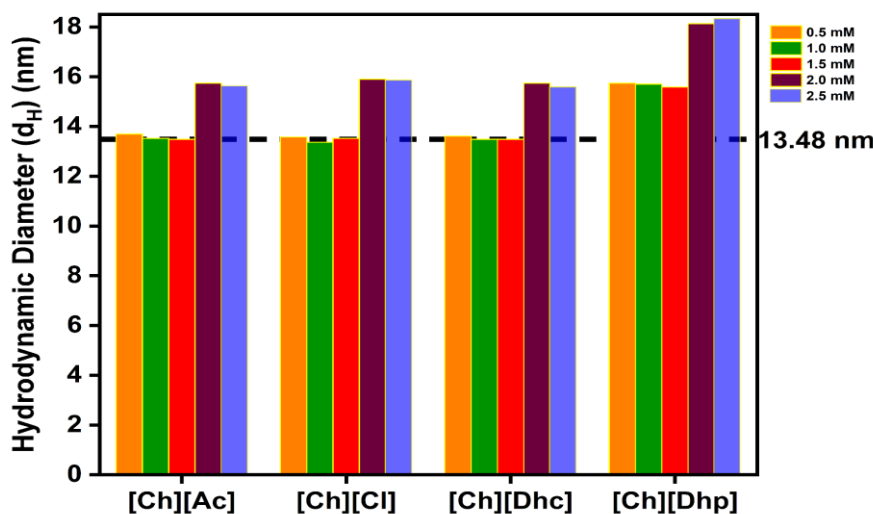


12 **Figure 10.** The hydrodynamic diameter ( $d_H$ ) analysis of IgG at 25 °C in the presence of  
13 phosphate buffer (pH=7.0, 10 mM) and at various concentrations of ILs: (a) [Ch][Ac], (b)  
14 [Ch]Cl, (c) [Ch][Dhc] and (d) [Ch][Dhp].

15  
16 The  $d_H$  value of IgG in phosphate buffer (Control) at pH 7.0 under physiological conditions was  
17 13.86 nm, which is in good agreement with reported data.<sup>41</sup> Figure 11 explicitly shows that the

1  $d_H$  values of IgG in all the ILs are not appreciably changed up to the concentration 1.5 mM. For  
 2 example,  $d_H$  values are 13.48, 13.52, 15.90, 15.86 for concentrations 0 (control), 1.0, 1.5, and 2.5  
 3 mM of [Ch][Ac] given in Figure 10 and 11. The ILs [Ch]Cl, [Ch][Dhp] and [Ch][Dhc], behave  
 4 in a similar fashion. Any slight increment in the  $d_H$  can be explained on the basis of an increase  
 5 in the number of ion-ion repulsions, which can be expected to increase the value of  $d_H$  in protein.  
 6 Therefore, it can be concluded that in the presence of all four ILs, IgG retains its compact  
 7 structure and shows no significant change in the  $d_H$  values as compared with the control whereas  
 8 there is increase in aggregation formation in case of [Ch][Dhp] explained by appearance of wider  
 9 peaks.

10



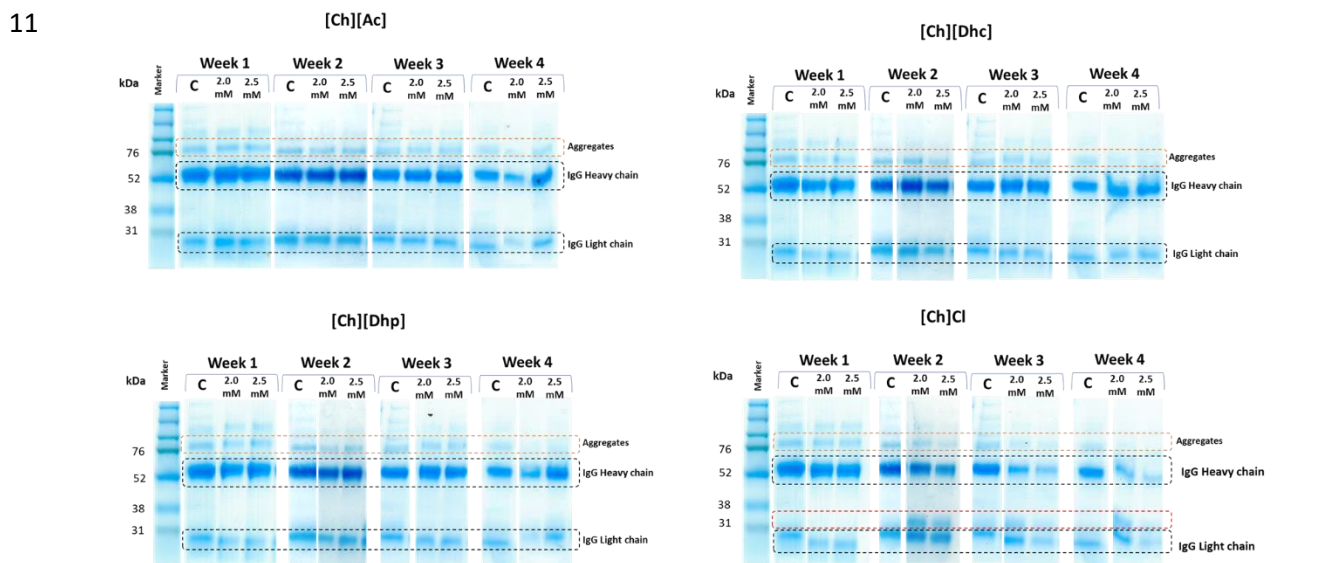
11 **Figure 11.** The hydrodynamic diameter ( $d_H$ ) at 25 °C for IgG in 0.5 mM (orange), 1.0 mM  
 12 (green), 1.5 mM (red), 2.0 mM (violet) and 2.5 mM (blue) [Ch][Ac], [Ch]Cl, [Ch][Dhc] and [Ch]  
 13 [Dhp]. The dashed line at 14.4 nm means the control (IgG in sodium phosphate buffer pH 7.0, 10  
 14 mM).

15

### 16 Time-dependent Stability Study of IgG in the Presence of Cholinium-based ILs

17 For studying the storage capability of IgG in different ILs, the SDS-PAGE, CD, and DLS  
 18 analysis of IgG in all the ILs was performed for four weeks at 2 and 2.5 mM concentration of  
 19 ILs.

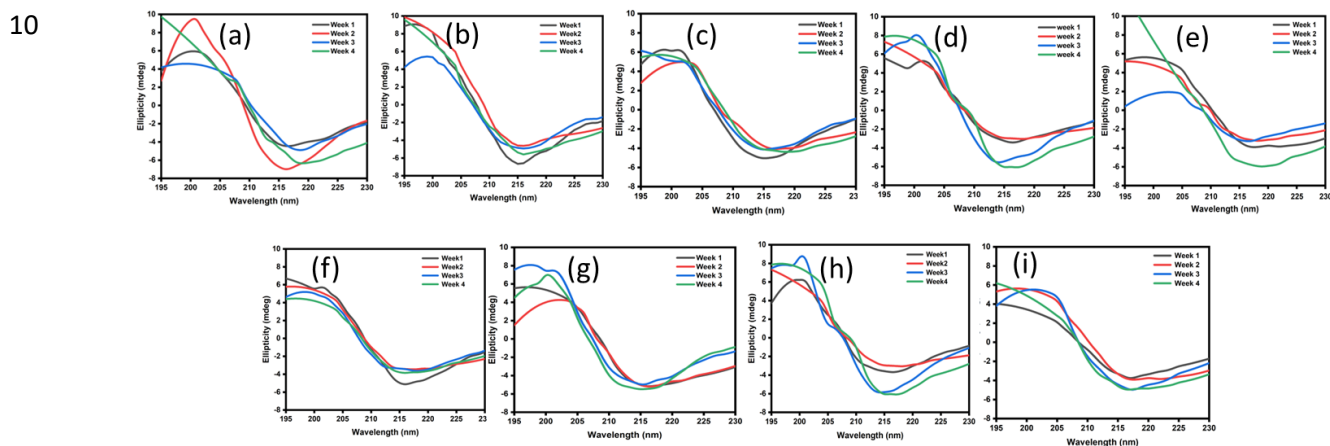
1 **SDS-PAGE Study:** The structural stability of IgG for four weeks in the presence of phosphate  
 2 buffer (control) and in the presence of [Ch][Ac], [Ch][Dhc], [Ch][Dhp] and [Ch]Cl at 2.0 and 2.5  
 3 mM was evaluated by SDS-PAGE in reduced conditions. The results depicted in Figure 12  
 4 shows that, except for [Ch]Cl, the light and heavy chains of IgG can be detected for both  
 5 concentrations and for the control after four weeks. For [Ch]Cl at both concentrations it is  
 6 possible to observe the presence of a new band at lower molecular weight after the second week  
 7 of incubation and a significant decrease in the intensity of IgG heavy chain when compared to  
 8 the control. These results indicate the reduction of aggregation of heavy chain of IgG in the  
 9 presence of [Ch]Cl after week 1. Thus, all the ILs are favorable to the structural stability of IgG  
 10 for a long period of time with [Ch]Cl being the favorable one.



12 Figure 12 - SDS-PAGE of IgG for four weeks of incubation at 25 °C in the presence [Ch][Ac],  
 13 [Ch][Dhc], [Ch][Dhp] and [Ch]Cl at 2.0 mM and 2.5 mM. Lane 1 – molecular weight marker;  
 14 lane 2 – IgG in sodium phosphate buffer pH 7.0, 10 mM (control (C)).

15 **CD Spectra Analysis:** To explore the long-term storage and possible structural changes of IgG,  
 16 far-UV CD studies were carried out in the presence of different cholinium based ILs, at 2 and 2.5  
 17 mM concentration for four weeks (Figure 13). As can be seen from Figure13 (a) IgG in  
 18 phosphate buffer (control) shows a signature peak of  $\beta$ -pleated at 218 nm up to 2weeks whereas,  
 19 on weeks 3 and 4, there is a blue shift of negative CD band which can be caused due to change in  
 20 the secondary structure of the IgG due to longer storage. Figure 13 (b) and (f) show the CD

1 spectra of IgG in [Ch][Ac] solution at concentration 2.0 mM and 2.5 mM and the result shows  
 2 that on week 4, there is a slight blue shift to the ellipticity values at concentration 2.0 mM  
 3 whereas at concentration 2.5 mM the structure is retained with a slight decrease in negative  
 4 ellipticity values. As can be seen from Figure 13 (c) and (g), the secondary structure of IgG in  
 5 presence of [Ch]Cl is more stable at 2 mM than 2.5 mM as peaks at 218 becomes wider at 2.5  
 6 mM on week 3 and 4 at higher concentration. Figure 13 (d) and (h) shows CD spectra of IgG in  
 7 [Ch][Dhc] at 2 mM and 2.5 mM respectively, as can be seen from spectra that on longer storage  
 8 the structure become destabilized, however, in case of [Ch][Dhp] IgG retained its structure at 2.5  
 9 mM on longer storage as compared to 2.5 mM.



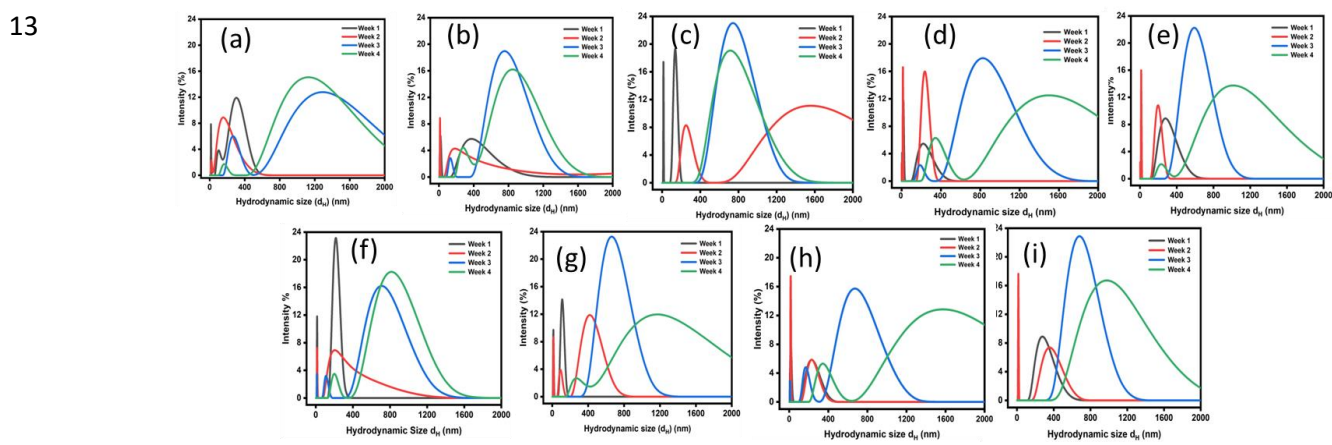
11 Figure 13. Far-UV CD analysis of IgG for four weeks at 25 °C in the presence of (a) phosphate  
 12 buffer (pH=7.0, 10 mM) alone, and at 2.0 mM (b) [Ch][Ac], (c) [Ch]Cl, (d) [Ch][Dhc] and (e)  
 13 [Ch][Dhp] and at 2.5 mM (f) [Ch][Ac], (g) [Ch]Cl, (h) [Ch][Dhc] and (i) [Ch][Dhp]

14

15 **Hydrodynamic size studies.** DLS was utilized to further observe the variation of  $d_H$  of IgG as a  
 16 function of time and the results are illustrated in Figure 14. The plot of size distribution by the  
 17 intensity of IgG in the buffer is displayed in Figure 14(a). One sharp peak at 13.95 nm has been  
 18 observed for IgG monomer while another peak at 313.2 nm has occurred due to the  
 19 oligomerization of the IgG monomer. . On week 2, the monomer's hydrodynamic size shifted to  
 20 higher-value that is 16.82 with low intensity and the second peak appeared at 155.6, showing the  
 21 increase in aggregation of the protein. After two more weeks, the protein samples were again



1 analyzed and two wider peaks can be seen that is the due formation of aggregates of the IgG.  
 2 Hence, it can be concluded that IgG is deactivated after 2 weeks of storage in buffer, which  
 3 causes the formation of higher aggregation. In [Ch][Ac] at 2.0 mM the aggregation pattern is  
 4 almost similar like in buffer alone whereas at 2.5 mM the  $d_H$  value is retained and the  
 5 aggregation decreases (as curves become sharper) for weeks 3 and 4, hence showing better  
 6 stability for long-term storage (Figure 14b). Whereas, [Ch]Cl displayed a decrease in aggregation  
 7 at both concentrations (Figure 14c). For [Ch][Dhc] the aggregation increases for week 3 and  
 8 week 4(Figure 14d). In presence of [Ch][Dhp] the aggregation is less pronounced as comparison  
 9 to the IgG in buffer alone solution. Hence, it can concluded that due to long-term storage the  
 10 aggregation IgG decreases in the presence of ILs with the sequence  
 11 [Ch][Cl]>[Ch][Ac]>[Ch][Dhp]>[Ch][Dhc]>buffer alone. All the DLS results are well consisted  
 12 with CD spectroscopic results.



14 Figure14. The hydrodynamic diameter ( $d_H$ ) analysis of IgG for four weeks at 25 °C in the  
 15 presence (a) phosphate buffer (pH=7.0, 10 mM) alone, and at 2.0 mM(b) [Ch][Ac], (c) [Ch]Cl,  
 16 (d) [Ch][Dhc] and (e) [Ch][Dhp] and at 2.5 mM (g) [Ch][Ac], (h) [Ch]Cl, (i) [Ch][Dhc] and (j)  
 17 [Ch][Dhp].

18 **Thermal Stability Analysis of IgG in Cholinium based ILs.** A protein-solvent system is a  
 19 thermodynamic system composed of the solute (i.e., the protein and the solvent (liquid water,  
 20 and buffer ions)). The native states and assemblies of the protein are stabilized by the  
 21 intermolecular and as well as intramolecular interactions of the protein in the solvent system.<sup>42</sup>  
 22 Hence, when we unfold a protein, the interior regions become exposed to the surroundings that



1 tend to change the thermodynamic forces that underlie the structure and function of the  
 2 biomolecules.<sup>43</sup> Thermodynamic parameters, free energy ( $\Delta G$ ) are useful in describing the global  
 3 protein folding phenomenon, and hence, is helpful in understanding protein stability whereas the  
 4 enthalpy change ( $\Delta H$ ), heat capacity change ( $\Delta C_p$ ), and transition temperature ( $T_m$ ) are helpful to  
 5 understand protein stability in terms of non-covalent forces of different structural states.<sup>44</sup> The  
 6 thermodynamic studies of denaturation of IgG were performed using a two-state mechanism as  
 7 shown in equation 1, where the native (N) is the folded state and the denatured (D) state is  
 8 unfolded state of the protein, and determined by thermal fluorescence.<sup>45</sup>

9 Sigmoidal fluorescence intensity curves were obtained for IgG in the presence of the various  
 10 concentrations of ILs. As indicated by equations (1) - (3) below, the fractions of folded protein ( $f_f$   
 11 ) and unfolded protein are ( $f_u$ ) are determined by combining the intensity,  $Y$ , of protein found at  
 12 a temperature,  $T$ , with the experimentally observed intensities of the pre-and post-transition  
 13 values, and, respectively, of the native and denatured  $Y_f$  and  $Y_u$  protein. The latter values are  
 14 obtained by extrapolating the pre-and post-transition baseline values using a linear fitting  
 15 method. Upon each change in temperature, the system is assumed to be at thermal equilibrium. It  
 16 is then possible to use equation 4 to define an effective equilibrium constant,  $K$ . This equilibrium  
 17 constant is related to the standard free energy of formation, according to eq 5. The melting  
 18 temperature can be defined by the condition,  $Y=1/2 ( Y_f+ Y_u )$ , for which  $K=1$  and  $\Delta_{fu} G =0$ .

19



21  $f_u = (Y_f - Y) / (Y_f - Y_u)$  (2)

22  $f_u + f_f = 1$  (3)

23  $K = f_u / f_f = (Y_f - Y) / (Y - Y_u)$  (4)

24  $\Delta_{fu} G = -RT \ln K$  (5)

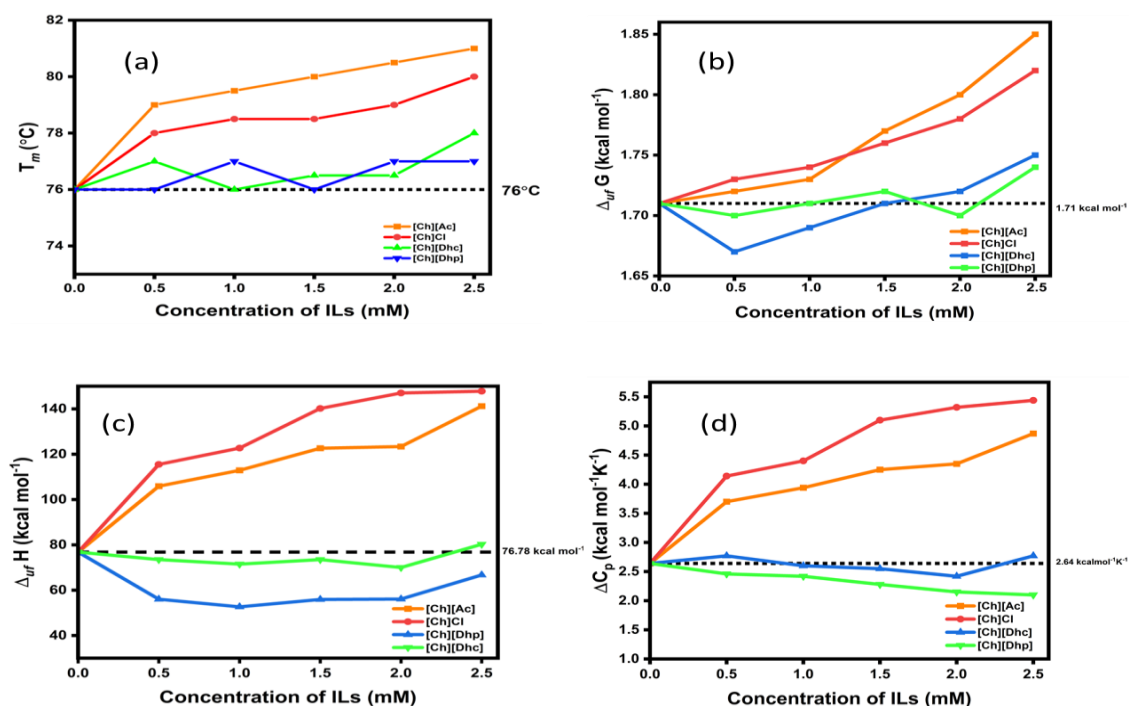
25  $\Delta_{fu} H = T_m \Delta_{fu} S$  (6)

26

1 If we let  $\Delta C_p$  represent the difference in the isobaric heat capacities of the two forms of the  
 2 protein, the integral of the Gibbs – Helmholtz equation leads to the result,

$$3 \Delta_{fu} G (T) = \Delta_{fu} H (T_m) [1 - (T/T_m)] + \Delta C_p [(T-T_m) - T \ln (T/T_m)] \quad (7)$$

4  
 5  
 6 The thermodynamic data obtained from the 25°C unfolding data are collected in Tables S5 and  
 7 S6. The intensity versus temperature data of sigmoidal curve of IgG in ILs are represented in  
 8 Figures S1-S4. All the obtained thermodynamic results are graphically depicted in Figure 15.



10 **Figure 15.** Effect of ILs on the thermal stability of IgG using fluorescence spectroscopy: (a)  
 11 transition temperature ( $T_m$ ); (b) Gibbs free energy changes ( $\Delta_{uf}G$ ); (c) enthalpy change ( $\Delta_{uf}H$ ) of  
 12 unfolding; and (d) heat capacity change of unfolding ( $\Delta C_p$ ) for IgG in presence of [Ch][Ac]  
 13 (orange), [Ch][Cl] (red), [Ch][Dhc] (blue) and [Ch][Dhp] (green). The dashed line shows the value  
 14 of control (IgG in sodium phosphate buffer, pH 7.0, 10 mM).

15 The results in Figure (15a) summarize the change of  $T_m$  values, which correspond to the  
 16 transition of IgG to the unfolded state, as a function of the ILs concentration. It can be seen that  
 17 in the presence of ILs, the  $T_m$  value of IgG was equal or exceeded the control point. In the

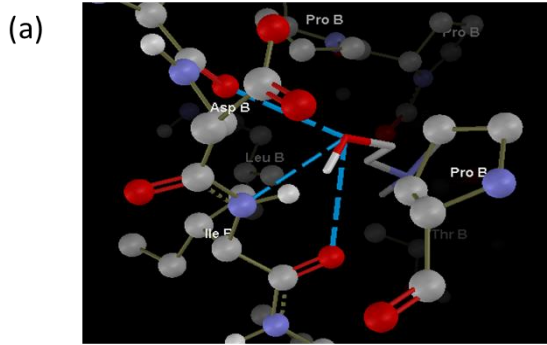
1 presence of [Ch][Ac], the  $T_m$  value of IgG increases linearly from 76 to 81°C with an increase in  
2 the IL concentration (0 to 2.5 mM). Similar is the case of [Ch] Cl, where the  $T_m$  value increases  
3 from 76 to 80 °C. For [Ch][Dhc] and [Ch][Dhp] there is no linear dependence of  $T_m$  of IgG with  
4 the concentration of IL; however, as mentioned earlier, in the presence of all ILs the  $T_m$  of IgG is  
5 always higher than in the control. Therefore, these observations evidently reveal that the IgG  
6 structure of the folded state is not altered by the addition of any studied IL and the stability  
7 abilities of the native state of IgG varies with the IL anion, following the trend: [Ch][Ac] >  
8 [Ch]Cl > [Ch][Dhc] > [Ch][Dhp]. Temperature is one of the main parameters; an increase in  
9 temperature causes the unfolding of the protein (antibody) and further aggregation. Hence,  
10 increase of any degree of transition temperature is beneficial for longer storage of the protein.

11 It emerges from Figure 15 (b, c and d) that the  $\Delta_{fu}H$ ,  $\Delta_{fu}G$  and  $\Delta C_p$  values of IgG in  
12 presence of [Ch][Ac] and [Ch]Cl increase linearly as the concentration increases. Perhaps there  
13 is an increment in the values of these parameters in the presence [Ch][Dhc] and [Ch][Dhp];  
14 however, the increment is below the control point. Therefore, the results from thermodynamic  
15 studies indicate that [Ch][Ac] and [Ch]Cl ILs interact unfavorably with the surface of IgG and  
16 that these ILs stabilize the folded native structure of IgG and do not interfere with the functional  
17 groups of IgG. On the other hand, [Ch][Dhc] and [Ch][Dhp] moderately interact with the surface  
18 of the protein, being slightly less favorable than [Ch][Ac] and [Ch]Cl.

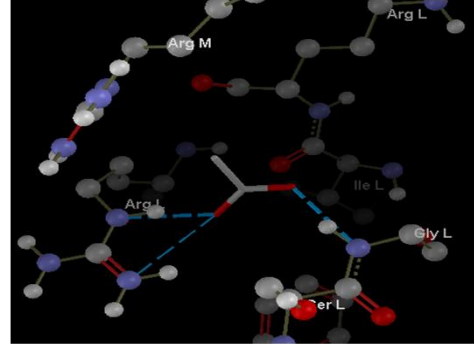
19 **Molecular Docking Studies.** Molecular docking was performed to study the potential binding  
20 sites of [Ch]Cl, [Ch][Ac], [Ch][Dhc] and [Ch][Dhp] at the  $F_{ab}$  and  $F_c$  fragments of IgG. There  
21 can be different types of interactions between  $F_{ab}$  and  $F_c$  fragments and ILs; however, for the  
22 sake of simplicity, only hydrogen bonding (H-bond) and hydrophobic interactions are studied  
23 under this section.

24

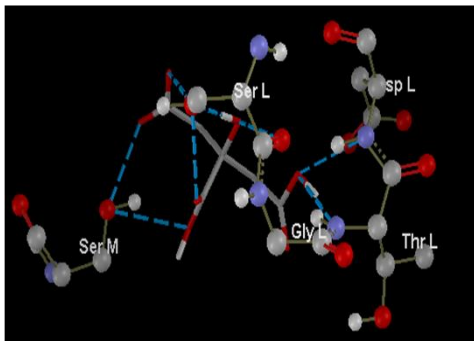
1



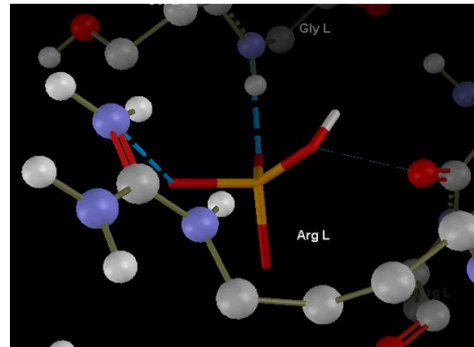
(b)



(c)

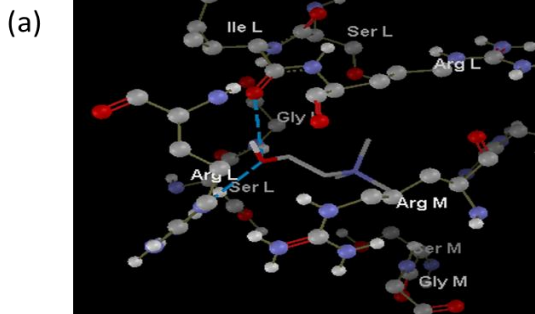


(d)

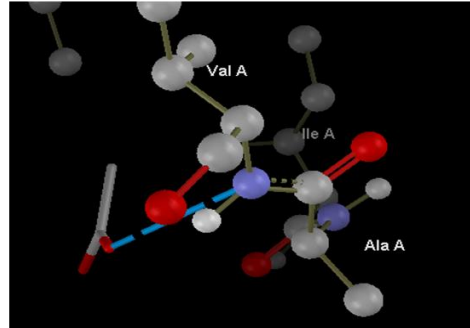


2 **Figure 16.** Molecular docking of F<sub>ab</sub> fragment with (a) cholinium cation; (b) acetate anion; (c)  
3 dihydrogen citrate anion; and (d) dihydrogen phosphate anion obtained from Molegro software.

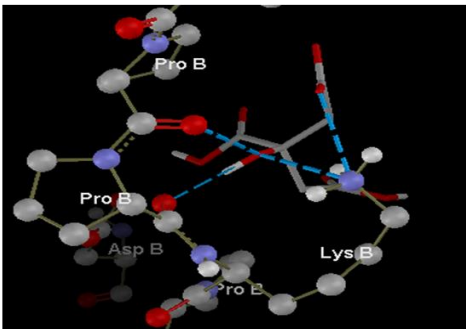
4



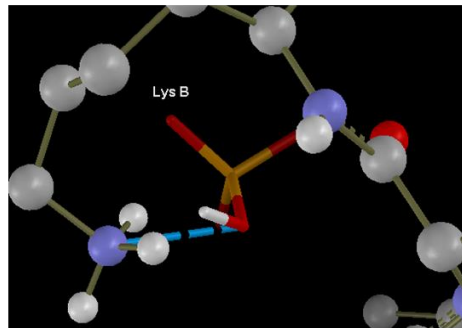
(b)



(c)



(d)



1 **Figure 17** Molecular docking of F<sub>c</sub> fragment with (a) cholinium cation; (b) acetate anion; (c)  
 2 dihydrogen citrate anion; and (d) dihydrogen phosphate anion obtained from Molegro software.

3 Figures 16 and 17 show the specific binding of cholinium, acetate, dihydrogen phosphate and  
 4 dihydrogen citrate ions with F<sub>ab</sub> and F<sub>c</sub> fragments of IgG through molecular docking. However,  
 5 the docking results for chloride could not be displayed as the Cl anion does not form a H-bond  
 6 with the protein molecules.<sup>46</sup> Figure 16 (c, d) and Figure 17 (c,d) show that hydrophobic  
 7 interactions in the case of dihydrogen citrate and dihydrogen phosphate are higher with three  
 8 amino acid residues of F<sub>ab</sub>, whereas three amino acid residues of F<sub>c</sub> fragments show hydrophobic  
 9 interactions with dihydrogen phosphate, which has also been seen in the FT-IR studies. Whereas  
 10 dihydrogen citrate is interacting with five hydrophobic residues of F<sub>ab</sub> and one hydrophobic  
 11 residue of F<sub>c</sub>, these interactions further explain the perturbation of the secondary structure of IgG  
 12 at higher concentrations of [Ch][Dhp] and [Ch][Dhc]. However, the strong binding of cholinium-  
 13 based ILs with IgG is evident by the formation of hydrogen bonds with F<sub>ab</sub> (Ile 28, Arg 31) and  
 14 F<sub>c</sub> (Ile 377) fragments with the cholinium cation. All further results are summarized in Table 1.

15 **Table 1:** Summary of molecular docking studies of F<sub>ab</sub> and F<sub>c</sub> fragments of IgG with cholinium-  
 16 based ILs.

Ions	Hydrogen bonding interactions		Hydrophobic interactions	
	F <sub>ab</sub>	F <sub>c</sub>	F <sub>ab</sub>	F <sub>c</sub>
Cholinium	Ile 28, Arg 31	Ile 377	Ile 28, Arg 31	Ser 375
Acetate	Arg 29, Arg 31	Arg 29, Arg 31	Lys 248	Lys 248
Dihydrogen Phosphate	Thr 69, Asp7, Ser 67		Thr 69, Asp70, Ser 67	Lys246, Pro 244, Pro 245
Dihydrogen Citrate	Ser 67, Ser 67, Asp 70, Thr 69	Lys 69	Ser 67, Ser 67, Asp 70, Thr 69, Gly 68	Lys 69

17

1 Spectroscopy has shown that the hyperchromic/hypochromic shift seen in UV and fluorescence  
2 spectroscopy has exhibited that IgG is more stable in the presence of [Ch][Ac] and [Ch]Cl,  
3 which is further verified by analyzing the secondary structure of IgG using Far-UV CD and FT-  
4 IR spectroscopy. The secondary structure of IgG has been retained in the presence of all the ILs;  
5 however, when comparing all the four ILs the trend of IgG secondary structure stability is as  
6 follows: [Ch][Ac] > [Ch]Cl > [Ch][Dhc] > [Ch][Dhp]. Furthermore, thermal denaturation studies  
7 showed that the  $T_m$  increases with increasing the concentration of ILs, denoting that the overall  
8 thermal stability of the IgG

9 Our parallel (UV absorbance, fluorescence, SE-HPLC, SDS-PAGE, far-UV CD, thermodynamic  
10 Fluorescence, DLS, FTIR and Molecular Docking) results show that cholinium-based ILs are a  
11 highly important class of excipients to be considered in IgG formulations. In general, the anion  
12 variation is thought to have a superseding effect on the structure and the stability of protein than  
13 that of the cation. The interactions between proteins and IL solutions are controlled by the  
14 complex interactions depending on some microscopic properties such as ion hydration, ion effect  
15 on protein hydration and direct interactions between ions and proteins. Our results have revealed  
16 that the effect of anions on the stability of protein seems to be much more complicated and does  
17 not always follow the Hofmeister series. Hence, the most promising ILs for IgG stability are  
18 [Ch][Ac] and [Ch]Cl.

19 Antibodies-mediated therapeutic drug stability depends on the distinct formulation environment  
20 and various excipients like arginine and arginine hydrochloride (ArgHCl), which are effective  
21 additives to improve protein stability.<sup>47</sup> Cholinium-based ILs are well known to improve proteins  
22 stability and their ability to extensively reduce aggregation, which makes them potential solvent  
23 additives for the formulation development of therapeutic proteins. Recently, Hallet and co-  
24 workers have studied the formulation consisting of [Ch][Dhp] and different excipients.<sup>18</sup> They  
25 have found that in the presence of [Ch][Dhp], the structure of IgG is less stabilized, although the  
26 destabilizing effect of [Ch][Dhp] is overcome by adding the excipients. Similarly, in our studies,  
27 [Ch][Dhp] is also not completely helping the IgG to retain its confirmation, whereas ILs like  
28 [Ch][Ac] and [Ch]Cl are potential solvent additives for the formulation development of IgG.  
29 These results reinforce the potential of cholinium-based ILs paired with appropriate anions to be  
30 considered as potential excipients of biopharmaceutical formulations.

31

## 1 CONCLUSIONS

2 Most of the studies on protein–IL mixtures have specifically targeted to enzymes. However,  
3 there is a range of protein-based biopharmaceuticals, such as IgG, in which ILs may play a  
4 relevant role in their stabilization. The present study delivered a comprehensive overview of the  
5 outcome of cholinium-based ILs on the stability and thermodynamic profile of IgG antibodies.  
6 The results indicate an appreciable increase (around 5 °C) in  $T_m$  values of IgG in presence of  
7 [Ch][Ac] (81 °C), [Ch]Cl (80 °C), [Ch][Dhc] (78°C) and [Ch][Dhp] (77 °C) as compared to  
8 buffer (76 °C). SE-HPLC and SDS-PAGE results have shown that cholinium-based ILs do not  
9 lead to the formation of IgG aggregates or IgG fragmentation. The spectroscopic studies  
10 concluded that [Ch][Ac] and [Ch]Cl are preferred ILs for providing the conformational and  
11 thermal stability of IgG. Time dependent studies of IgG have also been performed to study the  
12 effect of ILs on long-term stability and the results shows the high potential of ILs as storage  
13 media for IgG for longer period of time. Hence, from our study we can interpret that cholinium-  
14 based ILs can be explored more in future as these ILs have shown more structural and thermal  
15 stability of IgG. Taking a step forward, these ILs should be investigated to stabilize other  
16 relevant antibodies, like IgA and IgM, or other biopharmaceuticals. Finally, the required studies  
17 to validate their use in biopharmaceutical formulations must be conducted.

18

19

## 20 ASSOCIATED CONTENT

21

22 \*S Supporting Information

23

24 The Supporting Information is available free of charge at

25

26 water content and pH of ILs, the tables of UV-Vis spectroscopy, Fluorescence spectroscopy  
27 (values), Hydrodynamic size (DLS studies), Thermal fluorescence (Sigmoidal graphs of  $T_m$ ), all  
28 the thermodynamic parameters in buffer and in various concentration of ILs.

29

1  
2  
3  
4  
5  
6  
7  
8  
9  
10  
11  
12  
13  
14  
15  
16  
17  
18  
19  
20  
21  
22  
23  
24  
25  
26  
27  
28

## AUTHOR INFORMATION

### **Corresponding Authors**

**Mara G. Freire** - CICECO-Aveiro Institute of Materials, Department of Chemistry, University of Aveiro, 3810-193, Aveiro, Portugal, E-mail: maragfreire@ua.pt

**Pannuru Venkatesu** - Department of Chemistry, University of Delhi, Delhi 110007, India; E-mail: venkatesup@hotmail.com, pvenkatesu@chemistry.du.ac.in

### **Authors**

**Diksha Dhiman** - Department of Chemistry, University of Delhi, Delhi 110007, India

**Meena Bisht** - Department of Chemistry, University of Delhi, Delhi 110007, India

**Ana P. M. Tavares** - CICECO-Aveiro Institute of Materials, Department of Chemistry, University of Aveiro, 3810-193, Aveiro, Portugal

## CONFLICTS OF INTEREST

There are no conflicts to declare.

## ACKNOWLEDGEMENT

This work was developed within the scope of the project CICECO-Aveiro Institute of Materials, UIDB/50011/2020 & UIDP/50011/2020, financed by national funds through the Portuguese Foundation for Science and Technology/MCTES. P. V. gratefully acknowledges the Council of Scientific & Industrial Research (CSIR), New Delhi, India through Grant No. 01/3016/21/EMR-II for their financial support. Ana P. M. Tavares acknowledges the FCT for the research contract CEECIND/2020/01867. D.D. thanks the Council of Scientific and Industrial Research (CSIR), New Delhi for providing JRF (Junior Research Fellowship).

## ORCID

**Pannuru Venkatesu:** 0000-0002-2066-9807



1 **Mara G. Freire:** 0000-0001-8895-0614

2 **Ana P.M. Tavares:** 0000-0001-9128-6275

3

4 **REFERENCES**

5

6 1. Roque, A.C.; Lowe, C.R.; Taipa, M.A. Antibodies and genetically engineered related  
7 molecules: production and purification. *Biotechnol Prog.* **2004**, *20*, 639-654.

8 2. Vaillant, J.A.A.; Jamal, Z; Ramphul, K. Immunoglobulin. Treasure Island (FL), *StatPearl*,  
9 StatPearls Publishing, **2021**.

10 3. Janeway, C.A. Jr.; Travers, P.; Walport, M. Shlomchik, M.J. Immunobiology: The Immune  
11 System in Health and Disease. 5<sup>th</sup> edition, New York, *Garland Science*, **2001**.

12 4. Vermeer, A.W.; Norde, W.; The thermal stability of immunoglobulin: unfolding and  
13 aggregation of a multi-domain protein. *Biophys J.* **2007**, *8*, 394-404.

14 5. Takeda Pharmaceuticals U.S.A, GAMMAGARD LIQUID, Immune Globulin Infusion  
15 (Human) 10%, (n.d.). <https://www.gammagard.com/primary-immunodeficiency> (accessed  
16 November 5, 2021).

17 6. A. Biologics, ASCENIV, Immune Globulin Intravenous (Human), stra 10% liquid, (n.d.).  
18 <https://www.asceniv.com/about-pi.html> (accessed November 5, 2021).

19 7. Farid, S. S. Process economics of industrial monoclonal antibody manufacture. *J.*  
20 *Chromatogr. B.* **2007**, *848*, 8–18.

21 8. Wang, W.; Singh, S.; Zeng, D.L.; King, K.; Nema, S. Antibody structure, instability, and  
22 formulation. *J. Pharm. Sci.* **2007**, *96*, 1-26.

23 9. Rtner, H.W.; Christian, C.C.; How ionic liquids can help to stabilize native proteins. *Phys.*  
24 *Chem. Chem. Phys.* **2012**, *14*, 415-426.

- 1 10. Bisht, M.; Mondal, D.; Pereira, M. M.; Freire M. G.; Venkatesu, P.; Coutinho, J. A. P.  
2 Long-term protein packaging in cholinium-based ionic liquids: improved catalytic activity and  
3 enhanced stability of cytochrome c against multiple stresses. *Green Chem.* **2017**, *19*, 4900-4911.
- 4 11. Park, J.W. Comparison of stabilizing effect of stabilizers for immobilized antibodies on  
5 QCM immunoensors. *Sens. Actuat. B:Chem.* **2003**, *91*, 158–162
- 6
- 7 12. Allen, D. T.; Rosselot, K. S.; Pollution prevention for chemical processes: a handbook  
8 with solved problems from the refining and chemical processing industries. **1994**, University of  
9 California Los Angeles, Department of Chemical Engineering. TR Series (Hazardous Waste  
10 Research and Information Center), no. 22, The Center.
- 11 13. Ventura, S. P. M.; Silva, F. A. e.; Gonçalves, A. A. M.; Pereira, J. L.; Gonçalves, F.;  
12 Coutinho, J. A. P. Ecotoxicity Analysis of cholinium-based Ionic Liquids to *Vibrio fischeri*  
13 Marine Bacteria. *Ecotoxicol. Environ. Saf.* **2014**, *102*, 48–54.
- 14 14. Passino, D. R. M.; Smith, S. B. Acute Bioassays and Hazard Evaluation of  
15 Representative Contaminants Detected in Great Lakes Fish. *Environ. Toxicol. Chem.* **1987**, *6*,  
16 901–907.
- 17 15. Ventura, S. P.M.; Silva, F.A.; Goncalves, A.M.M.; Pereira, J.L.;Goncalves, F.; Coutinho,  
18 J. A. P. Ecotoxicity analysis of cholinium-based ionic liquids to *Vibrio fischeri* marine bacteria.  
19 *Ecotoxicol. Environ. Saf.* **2014**, *102*, 48-54.
- 20 16. Rantamaki, A. H.; Ruokonen, S. K.; Sklavounos, E.; Kyllonen, L.; King, A. W. T.;  
21 Wiedmer, S. K. Impact of Surface-Active Guanidinium-, Tetramethylguanidinium-, and  
22 Cholinium-Based Ionic Liquids on *Vibrio Fischeri* Cells and Dipalmitoylphosphatidylcholine  
23 Liposomes. *Sci. Rep.* **2017**, *7*, 1–12

24  
25

- 1 17. Bisht, M.; Jha, I.; Venkatesu, P. Comprehensive Evaluation of Biomolecular Interactions  
2 between Protein and Amino Acid Based-Ionic Liquids: A Comparable Study between  
3 [Bmim][Br] and [Bmim][Gly] Ionic Liquids. *Chemistry Select* **2016**, *1*, 3510-3519.
- 4 18. Kumar, P.K.; Bisht, M.; Venkatesu, P.; Bahadur, I.; Ebenso E.E. Exploring the Effect of  
5 Choline-Based Ionic Liquids on the Stability and Activity of Stem Bromelain. *J. Phys. Chem. B*  
6 **2018**, *122*, *46*, 10435–10444.
- 7 19. Bisht, M.; Venkatesu, P. Influence of cholinium-based ionic liquids on the structural  
8 stability and activity of a-chymotrypsin. *New J. Chem.* **2017**, *41*, 13902-13911.
- 9 20. Mondal, D.; Sharma, M.; Quental, M.V.; Prasad, K.; Tavares, A.P.M.; Freire M. G.  
10 Suitability of bio-based ionic liquids for the extraction and purification of IgG antibodies. *Green*  
11 *Chem.* **2016**, *18*, 6071-6081.
- 12 21. Shmool, T.A.; Martin, L.K.; Bui-Le, L.; Moya-Ramirez, I.; Kotidis, P.; Matthews, R.P.;  
13 Venter, G.A.; Kontoravdi, C.; Polizzi, K.M.; Hallett, J.P. An experimental approach probing the  
14 conformational transitions and energy landscape of antibodies: a glimmer of hope for reviving  
15 lost therapeutic candidates using ionic liquid. *Chem. Sci.* **2021**, *12*, 9528-9545.
- 16 22. Ramalho, C.C.; Catarina, M.S.; Neves, S.; Quental, M.V.; Coutinho, J.; A.P.; Freire,  
17 M.G. Separation of immunoglobulin G using aqueous biphasic systems composed of cholinium-  
18 based ionic liquids and poly(propylene glycol). *J. Chem. Technol. Biotechnol.* **2018**, *93*, 1931-  
19 1939.
- 20 23. Wang, C. Metal-organic framework as a protective coating for biodiagnostic chips. *Adv.*  
21 *Mater.* **2017**, *29*.
- 22 24. Islam, S.; Moinuddin, M.A.R.; Arfat, M.Y.; Alam, K.; Ali A. Fine characterization of  
23 glucosylated human IgG by biochemical and biophysical methods. *Int. J. Biol. Macromol.* **2017**,  
24 *104A*, 19-29.
- 25 25. Ramalho, C. C.; Neves, C.; Quental, M. V.; Coutinho, J.; Freire, M. G. Potential of  
26 aqueous two-phase systems for the separation of levodopa from similar biomolecules. *J. Chem.*  
27 *Technol. Biotechnol.* **2018**, *93*, 1931-1939.

- 1 26. Melo, E.P.; Aires-Barros, M.R.; Costa, S.M.; Cabral J.M. Thermal unfolding of proteins  
2 at high pH range studied by UV absorbance. *J. Biochem. Biophys. Methods.* **1997**, *34*, 45-59.
- 3 27. Fink, A.L. Protein aggregation: folding aggregates, inclusion bodies and amyloid.  
4 *Folding and Design* **1998**, *3*, R9-R23.
- 5 28. Hong, P.; Koza, S.; Bouvier, E. S. P. A review of size-exclusion chromatography for the  
6 analysis of protein biotherapeutics and their aggregates. *J. Liq. Chromatogr. Relat. Technol.*  
7 **2012**, *35*, 2923-2950.
- 8 29. Rawat, K.; Bohidar, H.B.; Heparin-like native protein aggregate dissociation by 1-alkyl-  
9 3-methyl imidazolium chloride ionic liquids, *Int. J. Biol. Macromol.* **2015**, *73*, 23-30.
- 10 30. Gao, H.; Renslo, A.R. A practical synthesis of differentially protected 2-  
11 (hydroxymethyl) piperazines. *J Org Chem.* **2007**, *72*, 8591-8592.
- 12 31. Lange, C.; Patil, G.; Rudolph, R. Ionic liquids as refolding additives: N'-alkyl and N'-( $\omega$ -  
13 hydroxyalkyl) N-methylimidazolium chlorides. *Protein Sci.* **2009**, *14*, 2693-270.
- 14 32. Ferreira, A.M.; Faustino, V.F.M.; Mondal, D.; Coutinho, J.A.P.; Freire, M.G.; Improving  
15 the extraction and purification of Immunoglobulin G by the use of Ionic liquids as adjuvants in  
16 aqueous biphasic systems. *J. Biotechnol.* **2016**, *236*, 166-175.
- 17 33. Lakowicz, J. R. Principal of fluorescence spectroscopy, 3<sup>rd</sup> edition, *Kluwer Academic/  
18 Plenum Publishers*, Maryland, USA. **2016**.
- 19 34. Jha, I.; Venkatesu, P. Unprecedented Improvement in the Stability of Hemoglobin in the  
20 Presence of Promising Green Solvent 1Allyl-3-methylimidazolium Chloride. *ACS Sustainable  
21 Chem. Eng.* **2016**, *4*, 413–421.
- 22 35. Geng, S.; Cui, Y.; Liu, Q.; Cui, F.; Zhang, G.; Chi, Y.; Peng, H. Spectroscopic and  
23 molecular modeling study on the interaction of ctDNA with 3'-deoxy-3'-azido doxorubic.  
24 *Journal of Luminescence*, **2013**, *141*,144-149.

- 1 36. Joshi, V.; Shivach, T.; Yadav N.; Rathore, B.A.S. Circular Dichroism Spectroscopy as a  
2 Tool for Monitoring Aggregation in Monoclonal Antibody Therapeutics. *Anal. Chem.* **2014**, *86*,  
3 11606–11613.
- 4 37. Greenfield, N. J. Using circular dichroism spectra to estimate protein secondary structure,  
5 *Nat. Protoc.* **2006**, *1*, 2876–2890.
- 6 38. Jackson, M.; Mantsch, H. The use and misuse of FTIR spectroscopy in the determination  
7 of protein structure. *Biochem Mol Biol* **1995**, *30*, 95–120.
- 8 39. Kong, J.; Yu, S. Fourier Transform Infrared Spectroscopic Analysis of Protein Secondary  
9 Structures. *Acta Biochim Biophys Sin*, **2007**, *39*, 549–559.
- 10 40. Gagnon, P.; Nian, R.; Leong, D.; Nian, A.H.; Hoi, D.L.A. Transient conformation  
11 modification of immunoglobulin G during purification by protein A affinity chromatography. *J.*  
12 *Chromatogr. A*, **2015**, *1395*, 136-142.
- 13 41. Parmar, A. S.; Muschol, M. Hydration and hydrodynamic interactions of lysozyme:  
14 effects of chaotropic versus kosmotropic ions. *Biophysical Journal* **2019**, *97*, 590–598.
- 15 42. Santoro, M.M.; Bolen, D. W.; A test of the linear extrapolation of unfolding free energy  
16 changes over an extended denaturant concentration range. *Biochemistry* **1992**, *31*, 4901–4907.
- 17 43. Attri, P.; Venkatesu, P.; Lee, M.J. Thermodynamic characterization of the biocompatible  
18 ionic liquid effects on protein model compounds and their functional groups. *J Phys Chem B.*  
19 **2010**, *114*, 1471-1478.
- 20 44. Kumar, A.; Rani, A.; Venkatesu, P. A comparative study of the Hofmeister series of  
21 anions of the ionic salts and ionic liquids on the stability of  $\alpha$ -chymotrypsin  
22 *New J. Chem.* **2015**, *39*, 938-952.
- 23 45. Kosa, T.; Maruyama, N.; Sakai, N.; Yonemura, S.; Otagiri, M.; Maruyama, T. Structural  
24 and Ligand-Binding Properties of Serum Albumin Species Interacting with a Biomembrane  
25 Interface *Pharm. Res.*, **1998**, *15*, 592–598.

1 46. Sindhu, A.; Bhakuni, K.; Sankaranarayanan, K.; Venkatesu, P. Implications of  
2 Imidazolium-Based Ionic Liquids as Refolding Additives for Urea-Induced Denatured Serum  
3 Albumin. *ACS Sustainable Chem. Eng.* **2020**, *8*, 604–612.

4 47. Maity, H.; O'Dell, C.; Srivastava, A.; Goldstein, J. Effects of arginine on photostability  
5 and thermal stability of IgG1 monoclonal antibodies. *Curr Pharm Biotechnol.* **2009**, *10*, 761-  
6 766.

7

8

9

10

11

12

13

14

15

16

17

18